

ULTRA LOW-COST INFRARED LASER FIBRE SYSTEM

Jake A. Carlino

Bachelor of Engineering

Major in Electronics Engineering



MACQUARIE
University
SYDNEY • AUSTRALIA

Department of Electronic Engineering
Macquarie University

November 6th 2017

Supervisor: Professor Stuart Jackson

ACKNOWLEDGEMENTS

I would like to thank my supervisor, Stuart Jackson first of all for the opportunity to participate in one of Bedrock Photonics research projects. I would also like to thank both Stuart Jackson and Robert Woodward for their valuable guidance and expertise given throughout the project. Without their help this work would not have been possible and I am truly grateful. I would like to thank the previous Bedrock Photonics researchers Emma Mujic, Elliot Cook and Thomas Ackroyd for providing most of the groundwork needed to comprehend and commence the project. Finally I would like to thank the current members of Bedrock Photonics for any aid they provided through the project, Matt and Greeshma Chamarchy.

STATEMENT OF CANDIDATE

I, Jake Carlino, declare that this report, submitted as part of the requirement for the award of Bachelor of Engineering in the Department of Electronic Engineering, Macquarie University, is entirely my own work unless otherwise referenced or acknowledged. This document has not been submitted for qualification or assessment at any other academic institution.

Student's Name: Jake Carlino

Student's Signature:

A handwritten signature in black ink, appearing to read 'Jake Carlino', written in a cursive style.

Date: 6/11/2017

ABSTRACT

Mid-IR photonics is an upcoming research field driven by the useful wavelength range from $2\text{-}20\mu\text{m}$ in the electromagnetic spectrum. In this range there are many important absorption wavelengths that are created and manipulated which are crucial in various applications relating to spectroscopy; some of these applications include security, chemical sensing, biological sensing and material processing. In particular the atmospheric transmission window from $3\text{-}5\mu\text{m}$, is which bedrock photonics has mainly focused its project ideas around. This project aims to develop a compact electro-optical system with low cost, commercial off-the-shelf subsystems that will power, cool and combine the narrowband visible light of a 520nm 1W green laser diode and a 660nm 500mW red laser diode. These beams of light will be combined using spectral beam combining techniques to increase beam output efficiency and then will be focused and sent through fibre optic cable which has been doped by some rare earth elements to achieve some form of superluminescence. The document will provide concepts and techniques used to accomplish the end product, background information relating to this project, procedures of the projects development and details on the potential of future development.

CONTENTS

1 Introduction.....	13
1.1 Motivation	14
1.2 Thesis Overview	14
1.2.1 Project Specifications	15
1.3 Project Baseline Review.....	15
1.3.1 Time Budget Review.....	15
1.3.2 Financial Budget Review.....	16
2 Background & related work	18
2.1 Spectroscopy in the Mid-infrared region	18
2.2 Semiconductor Laser Diodes.....	19
2.2.1 Electro-luminescence.....	20
2.2.2 Junction configurations	21
2.2.3 Input current and laser emissions	22
2.3 Laser diode current driving	23
2.4 Heat management.....	23
2.4.1 Laser diode operating conditions	23
2.4.2 Heat sinking.....	24
2.4.3 Thermo-electric air cooling system.....	27
2.5 Laser beam combining technique.....	29
2.5.1 Coherent beam combination	29
2.5.2 Spectral beam combination	29
2.6 Optical Alignment.....	30
2.7 Stimulated emissions in medium	32
2.7.1 Superluminescence.....	34
3 System model and Development.....	36
3.1 LPC-840 improvised components	37
3.2 Driver Calibration.....	38
3.2.1 LPC-840 dummy load.....	38
3.2.2 NDG7475 dummy load	39
3.2.3 LPC-840 improvised heat sink.....	40
3.3 Component Testing, Calibration and Connections.....	40

3.3.1 Component Testing.....	40
3.3.2 Components Utilized	42
3.4 Laser Diode Testing	43
3.4.1 LPC-840 Distance Test.....	43
3.4.2 LPC-840Close Range Test.....	44
3.4.3 NDG7475 Close Range Test.....	45
3.4.4 NDG7475 Distance Test.....	46
3.4.5 Beam Divergence and Collimation Testing.....	46
3.5 Optical Alignment Procedures	47
3.5.1 Focussing Lens Efficiency Tests.....	49
3.6 Fibre coupling.....	51
3.6.1 SMF-28	51
3.6.2 Holmium doped ZBLAN fibre - 0.5m.....	52
3.7 Single diode as pump source in Ho ZBLAN fibre.....	54
3.7.1 660nm diode as pump source in Ho ZBLAN - 1m.....	54
3.7.2 520nm diode as pump source in Ho ZBLAN fibre - 1m	56
4 Conclusions & Future Work.....	59
4.1 Discussion.....	59
4.2 Future Work	60
5 Appendix.....	62
5.1 Datasheets	62
5.1.1 LPC-840.....	63
5.1.2 NDG7475	64
5.1.3 W1209.....	65
5.1.4 DB650-50-500-12V-BL-LM.....	66
5.1.5 DB-12V-200-3500-GD-LM.....	67
5.1.6 12V-150-500-LD.....	68
5.1.7 5V-200-800-GD-RD.....	69
5.1.8 LM2596 STEP DOWN REGULATOR.....	70
5.1.9 TEC1-12706 COOLING PLATE.....	71
5.1.10 Corning SMF-28.....	72
5.1.11 Holmium ZBLAN.....	74
5.1.12 FB3000-500	75
5.1.13 LM317 current-limiter circuit	76
5.2 Consultation Meetings Attendance Form	77

6 Bibliography	78
-----------------------------	-----------

LIST OF TABLES

Table 1.1: Components list.....	17
Figure 2.1: Absorption spectra for the 5 gas species in the mid-infrared region. [8]	19
Figure 2.2: cut-away view of laser diode can [9]	20
Figure 2.3: Semiconductor laser construction [11]	21
Figure 2.4: Junction formats - LED (left), SOA (middle), LD (right)[7]	22
Figure 2.5: An example of how temperature effects current Vs output power[7]	24
Figure 2.6: Example of LD temperature on emission wavelengths. [12].....	24
Figure 2.7: TEC system breakdown	28
Figure 2.8: Dichroic mirror (left), Coherent and Spectral beam combining (right)	30
Figure 2. 9: Optical breadboard/Table used to support systems used for laser and optics related experiments, engineering and manufacturing.	31
Figure 2. 10: LineTool.co ALH 3 axis linear translation stage device used for precision alignment which includes M3 threaded holes for bracket systems.	31
Figure 2. 11: XYZ 3 Stage - course/fine Fibre Aligner	32
Figure 2.12: Stimulated emission in doped fibre.....	33
Table 3. 1: Focussing Lens efficiencies.....	50
Table 3.2: Launch efficiencies of light into smf-28.....	52

LIST OF FIGURES

Figure 1.1: Project Gantt chart.....	16
Figure 2.1: Absorption spectra for the 5 gas species in the mid-infrared region. [8]	19
Figure 2.2: cut-away view of laser diode can [9]	20
Figure 2.3: Semiconductor laser construction [11]	21
Figure 2.4: Junction formats - LED (left), SOA (middle), LD (right)[7]	22
Figure 2.5: An example of how temperature effects current Vs output power[7]	24
Figure 2.6: Example of LD temperature on emission wavelengths. [12].....	24
Figure 2.7: TEC system breakdown	28
Figure 2.8: Dichroic mirror (left), Coherent and Spectral beam combining (right)	30
Figure 2.9: Optical breadboard/Table used to support systems used for laser and optics related experiments, engineering and manufacturing.	31
Figure 2.10: LineTool.co ALH 3 axis linear translation stage device used for precision alignment which includes M3 threaded holes for bracket systems.	31
Figure 2.11: XYZ 3 Stage - course/fine Fibre Aligner	32
Figure 2.12: Stimulated emission in doped fibre.....	33
Figure 3.1: Schematic diagram of laser combiner system.	36
Figure 3.2: Wiring diagram of Current Limiter Circuit.	37
Figure 3.3: LM317 Limiter Circuit.....	38
Figure 3.4: LPC-840 dummy load	39
Figure 3.5: NDG7475 dummy load	39
Figure 3.6: (left) Heat sink with diode, (right) Diode in heat sink, driver and power supply connected. 40	
Figure 3.7: Collimated NDG7475 (left), LPC-840 (right)	41
Figure 3.8: Basic wiring diagram	43
Figure 3.9: Power and current relationship for the LPC-840 with and without a lens at a distance of 500mm.....	44
Figure 3.10: Power and current relationship for the LPC-840 with and without a lens	45
Figure 3.11: Power and current relationship for NDG7475 with and without a lens	45
Figure 3.12: Power and current relationship for the NDG7475 with and without a lens at a distance of 500mm.....	46
Figure 3.13: Aligned electro-optical system with labelled components.....	48
Figure 3.14: Coaxial beams near (Left), Coaxial beams far (Right).....	49
Figure 3.15: Red light in smf-28 (left), Green (middle), Combined (right).....	51
Figure 3.16: Combined light in Ho ZBLAN fibre with observable luminescence.....	53
Figure 3.17: OSA reading from 2700nm - 3000nm.....	54

Figure 3.18: 660nm single pump source and fibre aligned for maximum absorption	55
Figure 3. 19: 1 - 1.4 μm spectrum from 660nm pump source linear scale (left), log scale (right)	55
Figure 3. 20: Closer inspection of 1150nm wavelength emissions - linear scale (left), log scale (right)	56
Figure 3.21: The 1.5 - 3.4 μm spectrum (left), closer inspection of 2870nm emissions (right) - linear scale	56
Figure 3. 22: Single 520nm pump source in fibre	57
Figure 3. 23: Linear scale 650 - 1400nm absorption spectrum (left), log scale (right).....	57
Figure 3. 24: Closer inspection of 1150nm wavelength linear scale (left), log scale (right)	58
Figure 3. 25: The 1.5 - 3.4 μm absorption spectrum in linear scale (left), closer inspection at 2850nm log scale (right).....	58

LIST OF ABBREVIATIONS AND ACRONYMS

LD	Laser diodes
LED	Light emitting diode
TEC	Thermo-electric cooling
LAS	Laser absorption spectrometry
IR	Infrared
PSU	Power supply unit
EMF	Electromagnetic field
EMI	Electromagnetic interference
SBC	Spectral beam combining
CBC	Coherent beam combining
EFL	Effective focal length
OSA	Optical spectrum analyzer
NIR	Near infrared
MIR	Mid infrared
Ho	Holmium

1 INTRODUCTION

The fictitious start-up company "Bedrock Photonics" have thought to undergo a project that will exploit the electromagnetic spectrum by developing a device from commercial off-the-shelf materials that will produce broadband IR light and may in future work be used in field application. The project will involve many tasks the first includes the configuration of laser drivers, to achieve maximum possible output power of the laser diodes safely. The laser drivers mentioned regulate current and are used specifically because of laser diodes functional properties, when a diode reaches its operating voltage the main factor in the output power is the current, so any voltage increases from after this point will tend draw increasingly large amounts of current. A reminder that Ohms law states "current is directly proportional to voltage" therefore if there are any voltage spikes, current will also increase and can destroy the diodes. The lasers being used incorporate a 660nm 400mW diode and a 520nm 1W diode where the two output beams will be made coaxial through the process of spectral beam combination, which helps with increasing beam efficiency as well as intensity. Another task involves the construction of a thermal management system, this is a key subsystem in the project as laser diodes tend to accumulate heat quite quickly, the system will regulate the temperature of the diodes and ventilate any emissions so optimal operating conditions are taken advantage of. The integration of a fibre coupling system will be implemented in the electro-optical system to be used in conjunction with the combined narrowband visible light the diodes produce, this is one of many crucial steps to achieve light close to the mid-IR region, the optical medium with the correct subsystems will act as a gain hopefully providing some form of electromagnetic radiation in the mid infrared range. The project will incorporate concepts and ideas from two previous students work relating to the tuneable fibre laser Bedrock Photonics has already manufactured. This will act as a foundation of knowledge to help achieve the requirements of this project. Professor

Stuart Jackson will be supervising the project as the completion will provide research towards areas relating to mid-IR spectroscopy.

1.1 Motivation

As mentioned photonics in the mid-IR region is a under-utilised and diverse field of research which presents many potential applications in everyday life. The region refers to the 2.5-5 μm atmospheric window where with technological advances, can allow manipulation of the spectrum to be achieved without the need for excessively expensive materials and equipment. As it's known this part of the spectrum contains a wide variety of some of the most common molecules on earth that is subject to laser absorption. The most commonly known for example would be H_2O or water, a device that could exploit the wavelength that corresponds to water through absorption can be used in various applications relating to industry, science and medicine. Through a technique called "laser absorption spectrometry" which incorporates energizing of the molecules, a device can be used for things that include environmental sensing, bomb detection and even breathe analysis in medical applications. Furthermore a cheap and effective realization of combining the two laser diodes visible light will not only provide increased output power but also beam quality which can only lead to improved device functionality in the end product. Needless to say cheap field effective devices that incorporate the electro-optic system mentioned that can produce any infrared light are non-existent; therefore it provides the perfect opportunity for marketing potential to develop the device in question.

1.2 Thesis Overview

This chapter provides the basic concepts and motivation relating to the project; it describes what is to be expected for an end product and the various applications it could be used for. It provides an up to date financial budget with component listings and a time budget review as well as the project specifications for the device. The specifications had modified over the course of time due to inaccessibility to some components and device functionality, these modifications were reviewed and agreed upon by Stuart Jackson who is supervising the project's completion. Chapter 2 involves all related works used in this project whether it may be from previous student's projects or relevant research that relate to the project which typically involve the background theory behind a few concepts used throughout the projects process. Chapter 3 provides details on the development process of the device i.e. steps taken to construct the

subsystems, how the subsystems were integrated into the device, system models and schematics drawn and it incorporates measured test results of both the prototype and final product. Finally chapter 4 entails a summary of the report; it provides a discussion and information on future work with recommendations for improvements.

1.2.1 Project Specifications

The mentioned specifications were established at the start of the project which was agreed upon by Stuart Jackson:

- The systems various components and materials will have to be easily accessible to anyone and be minimal cost on all parts. Materials used are not only limited to those purchased but also parts salvaged from deconstructed items.
- The system needs to have an internal heat management system that must control any temperature increases produced from the diodes, it should achieve this by maintaining the appropriate temperature value required for the diodes to operate correctly and safely through either heat sinking or introducing TEC, it will also perform the task of ventilating any unwanted ambient air inside the device caused by components.
- A optical system that will incorporate the correct alignment, positioning of components and angling of mirrors that will successfully combine the two laser diode outputs.
- The system will introduce a cheap method of focusing the combined output light and send it through optical fibre for experimental use.

1.3 Project Baseline Review

The project had initiated its work on the 27th of July and was set to be completed prior the 6th of November. The financial budget allocated for this project is \$300 not including the parts already purchased essential to the project. The baseline has been created with the intention for 4 days of work each week.

1.3.1 Time Budget Review

Referring to Figure 1.1 the project was running behind schedule on the initial testing & comparison phase, this is only due to the parts essential to safely test the diodes without overheating and destroying them are being shipped in from overseas, there is no place in Australia that currently produces heat sinks for the diodes of the TO-18 or TO-5 diameter or

laser drivers. Nevertheless an improvised heat sink was designed as well as a corresponding limiting current circuit to aid in the gathering of specifications for the LPC-840 diode; this nevertheless was only a substitute and will not be used in the final product. However now that components did arrive the project navigated back on schedule, looking again at Figure 1.1. The projected timeline and the actual time taken on each phase can be seen under each task, the project did not finalise the product as expected however critical research questions relating to a number of the projects specifications were answered.

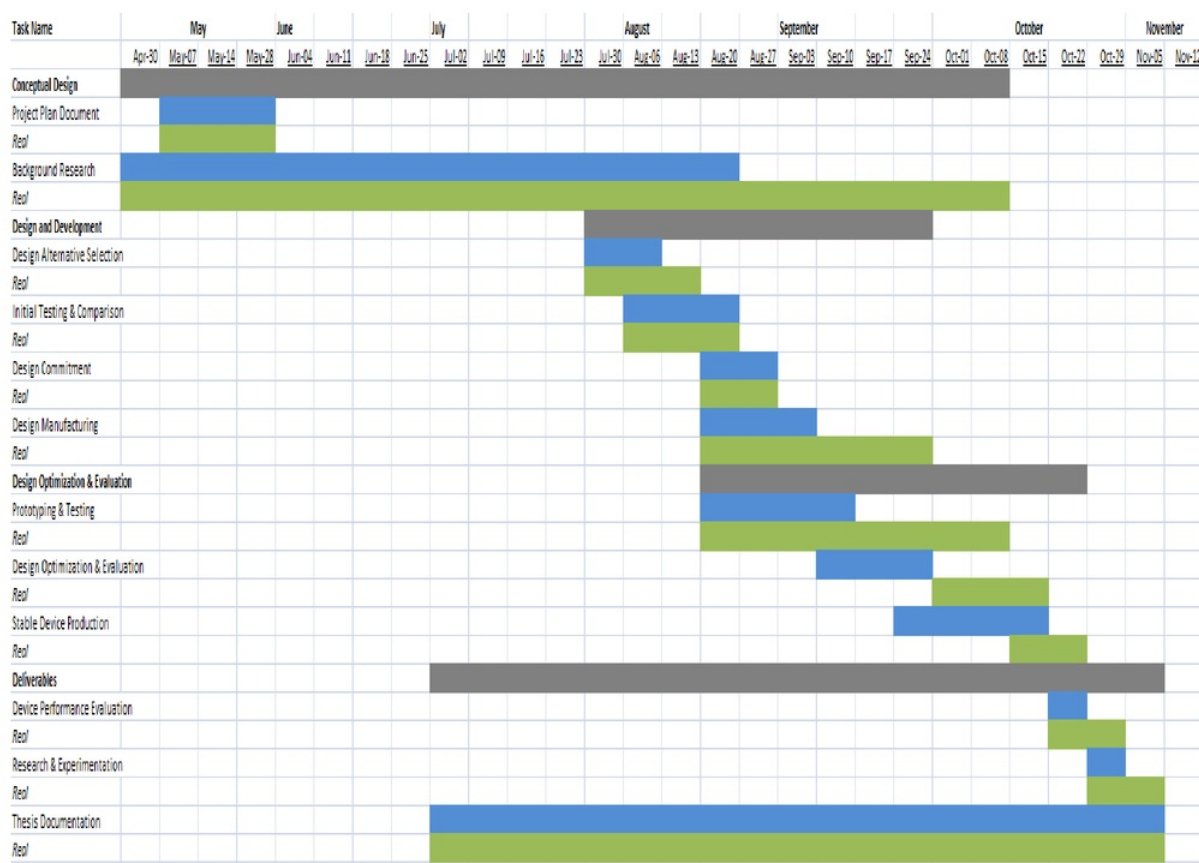


Figure 1.1: Project Gantt chart

1.3.2 Financial Budget Review

In accordance to the all materials purchased for use in the project, Table 1.1 shows approximately \$128AUS used; this includes all major components needed for the project. Many

components needed were salvaged from various appliances and previous projects, equipment such as soldering irons, power supplies, prototype boards and leads were also provided in the lab and had no contribution to cost. This also does not include the costs required to design and build the bracket mounts from METS for the 3 axis translational stage alignment components. Most of the components are also being shipped from Shenzhen, China which requires no postage fees and can be transitioned for free.

Item I.D	Description	Source	Price
TEC1-12706	2 x 12v 60W Thermoelectric cooler Peltier	Ebay	\$8
DB650-50-500-12V-BL-LM	2 x 12v 660nm 500mW Laser driver	Lazer-Makers Shenzhen, China	\$45
DB-12V-200-3500-GD-LM	1 x 12v 520nm 3500mW Laser driver	Lazer-Makers Shenzhen, China	\$25
Housing-650AL-LM	1 x TO-18 Heat sink + ost module w/ 12v fan& 660nm lens	Lazer-Makers Shenzhen, China	\$20
N/A	1 x TO-5 Heat sink + Host module w/ fan & 520nm lens	AptLightingWorld Shenzhen, China	\$20
LM4596	4 x DC-DC Step Down adjustable regulators	Ebay	\$10
Total	\$128.00		

Table 1.1: Components list

2 BACKGROUND & RELATED WORK

Chapter 2 provides detailed concepts and techniques used to accomplish each subsystem throughout the project. It provides information on works provided by others that relate to the project in some aspect. Most information and material used and directly referenced from other people's work provided a foundation of knowledge to gain a basic understanding of concepts relating to the different research fields incorporated in the project.

2.1 Spectroscopy in the Mid-infrared region

Spectrometry in the Mid-IR region as stated is bedrocks photonics main focus of research, work completed by Thomas Ackroyd, Elliot Cook and Emma Mujic provide material relating to the bedrock photonics project "A high power, tuneable Mid-IR, fibre laser", specifically Emma Mujic[1] investigates the applications of the $3\mu\text{m}$ wavelength created by fibre laser systems and references their uses from the following articles [2][3] [4] [5] [6] . In summation, applications for the $3\mu\text{m}$ wavelength can be used in a variety of fields such as tissue ablation with minimised unintentional damage and carbonisation, gaseous detection, tuned frequency probing of materials to characterise their molecular content, and O-H containment detection and characterisation [7] . As its seen research fields relating to medicine, industry and science have beneficial use of spectrometry in the Mid-IR field, furthermore Mujic also explains in her paper that while mid-infrared fibre laser systems do in fact exist, they are usually costly devices which have not been commercialised and are usually used for one specific purpose. The devices in question are

usually delicate and the market for wide application, field effective devices such as the tuneable fibre laser or this laser beam combiner is therefore a suitable and justifiable pursuit [7]

Furthermore spectroscopic research is designed so radiant energy interacts with specific types of matter; these types of matter include atoms, molecules, nuclei, crystals and extended materials alike. An example of a device technique that exploits the mid-infrared region is called laser absorption spectrometry. The technique uses the output laser wavelength to measure the concentration of group that is still in its gas phase. In physics absorption of electromagnetic radiation is the way in which the energy of a photon is taken up by matter. Laser absorption spectrometry itself has become the leading technique for gauging molecules and atoms as a gas type, a notable advantage of LAS is the ability to provide absolute assessment of the species under detection however a disadvantage of LAS is linked to how sensitive the optical system is when performing this task. If any noise is established during the assessment process, the sensitivity of the technique will decline and assessment reliability will be defective.[7]

Looking at Figure 2.1 it is evident of the relative absorption of compounds in the mid-infrared region. In this project techniques of laser combination with specifically chosen semiconductor diodes will be used in conjunction to achieve a goal of increased output efficiency. This output set up with particular optical subsystems may be able to achieve some sort of spectrometry in the mid-infrared region, such as laser absorption spectrometry as previously described.

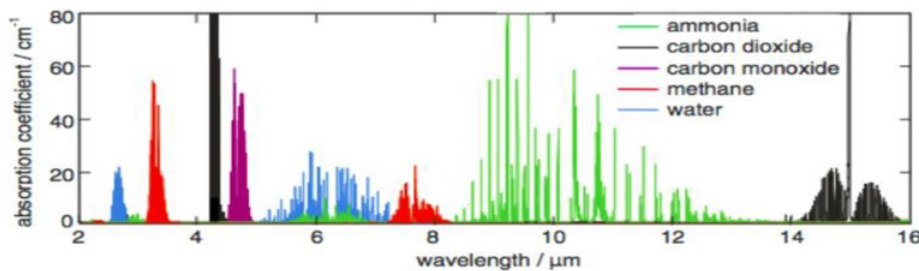


Figure 2.1: Absorption spectra for the 5 gas species in the mid-infrared region. [8]

2.2 Semiconductor Laser Diodes

The project's semiconductor essentials focus around two laser diodes for the light source. It will include one LPC-840, which will produce a 660nm wavelength and should produce an output power of up to 200mW, the device will also include one NDG7475 a high power semiconductor capable of outputting 1 watt at a 520nm wavelength. The light from both diodes will start as visible narrowband light, the NDG7475 generating a green beam and red from the LPC-840.

Looking at Figure 2.2 the basic structure of a laser diode can be seen, the device is a small chip bonded to a heat sink; tiny wires connect the chip for external use. Typically most of the light emitted by the laser comes out the front facet, where a small amount also comes out the back facet. The main laser light, usually elliptical and strongly diverging without a lens, comes out a window from the front of the semiconductor can [9]

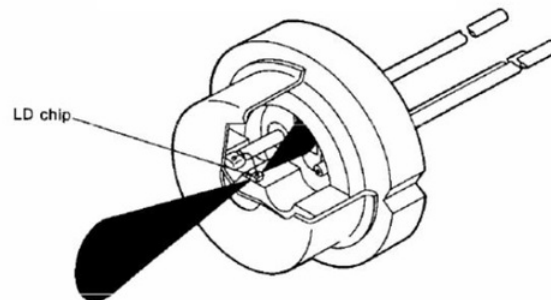


Figure 2.2:cut-away view of laser diode can [9]

The article [10] provides essential information relating to the semiconductor device functionality, Elliot Cooks [7] summary on the article suggests laser diodes and LEDs are very similar in operation. Given a forward biasing current is injected into the device's p-n junction a electron energy decay reaction would occur resulting in photon emissions. The difference between the two is that when an LED's electron energy decay reaction occurs the decays occur spontaneously and the photons created are out of phase. Whereas for the same reaction in the laser diode the decays are 'stimulated', by other light that has been created in the junction causing the total emissions to be polarised and in phase.

2.2.1 Electro-luminescence

Electroluminescence is usually achieved through the electron-hole recombination concept that occurs in certain semiconductor materials. The concept explains how light is achieved in semiconductor diodes due to the energy emitted by an electrons energy loss or 'decay' to get to a lower energy level. Energy is first introduced to the semiconductors junction, this causes that electrons energy levels to rise and hence gives it that potential to decay. One of the most common applications which involve this concept is to forward bias a p-n junction of a semiconductor, this is also known as injection electro-luminescence.

Very similar to what was mentioned above, when a forward voltage meets its threshold and energy is introduced through the p-n junction (in this case current), the electron and holes are forced towards the p-n junction and begin to combine. The positive or p-type materials in this

case have a large amount of holes and the n-type an excess of electrons. The electrons in the junction move from low energy to high energy levels due to the current. However before an electron and hole can combine a loss of energy from the electron is required to reach the lower energy level of the hole. This electron decay produces a photon in the p-n junction, in turn this stimulates more carriers in the semiconductor to combine thus leading to an increase in photons until the junction is filled and the output light is produced [11] ; Figure 2.3 shows the basic structure of the semiconductor and helps grasp the concept of what was explained.

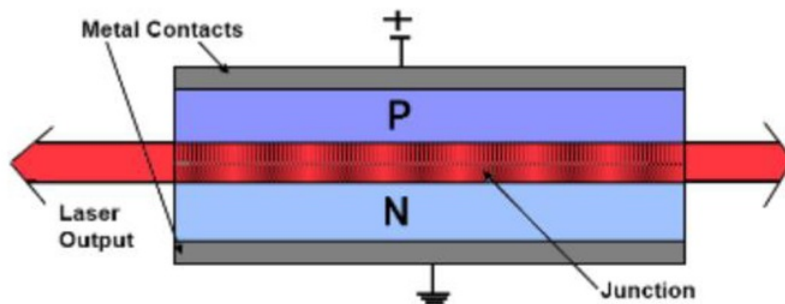


Figure 2.3: Semiconductor laser construction [11]

2.2.2 Junction configurations

In Cooks paper [7] he talks about the different type of electroluminescent photon configurations, the three basic types have been depicted in Figure 2.4. The junction can be used as a simple light source or as a semiconductor optical amplifier which injects photons into the forward biased junction to amplify the optical signal directly [10] .

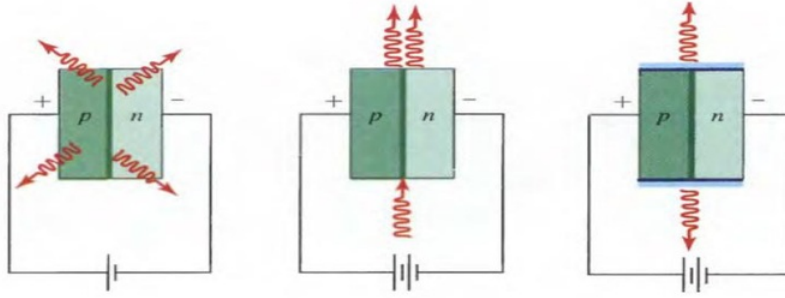


Figure 2.4: Junction formats - LED (left), SOA (middle), LD (right)[7]

2.2.3 Input current and laser emissions

Article [10] also explains how injection current is a key aspect in laser emission characteristics. Elliot Cook in addition encapsulates the main points relating to this in his paper [7]. Essentially there are four efficiencies associated with the semiconductor injected laser: The internal quantum efficiency

$$(1) \quad P = \eta_i(i - i_t) \frac{1.24}{\lambda_0}$$

which accounts for the actuality that only a fraction of the electron-hole recombination's are radiative in nature; there is the emission efficiency

$$(2) \quad \eta_e = \eta_d \left(1 - \frac{i_t}{i}\right) \frac{hv}{eV}$$

which accounts for the fact that only a portion of the light lost from the optical cavity is actually useful; the external differential quantum efficiency

$$(3) \quad \eta_d = \eta_e \eta_i$$

which accounts for both of these effects; and finally the power conversion efficiency

$$(4) \quad \eta = \eta_d \left(1 - \frac{i_t}{i}\right) \frac{hv}{eV} = \frac{P_o}{P_i}$$

which of course is the overall efficiency. The article states laser diodes often have power-conversion efficiencies around 50% which is well below the standard rating for other types of lasers. The main problem with this characteristic is that the energy that is not turned into photons is instead turned into phonons (heat), to deal with this the semiconductor devices are usually

mounted on or incorporated in some form of heat sink that helps dissipate the heat produced and stabilize temperature levels [10] .

2.3 Laser diode current driving

As it's known voltage and current spikes occur in electronic circuits in live conditions, laser diodes are known to be "current hungry devices" and it is required that a stable injection of current from the power supply is maintained. LD's tend to be extremely sensitive to the smallest fluctuations in voltage, these fluctuations would result in large alterations in current and therefore a large change of all operating characteristics. This is why current is regulated rather than voltage, if a voltage spike were to occur, even on a minute scale, current being directly proportionate to voltage would also fluctuate and the diode would draw an increasingly large amount of current at certain fluctuation points and destroy itself in the process. Article [12] points out how accuracy, stability and quality of the drive current largely effects multiple characteristics of the laser diodes output. It also discusses how and why linear regulation circuitry is best used to maintain current as well as discussing the use of grounded shielding cabling for EMI protection and finally a method of shorting the anode and cathode of an LD to prevent charge build-up from EMF and static. Cook[7] also refers to article [12] and concludes parallel findings.

2.4 Heat management

2.4.1 Laser diode operating conditions

Photonic output power of a laser diode is directly proportionate to input power supplied, knowing this we are able to calculate waste phonon created by the diode at maximum power and select an appropriate heat management system to disperse this waste. The conversion efficiency for the LPC-840 and NDG7475 have not been provided on the data sheets, So calculations will be performed to estimate the efficiencies of both diodes. As heat is created and component temperatures increase, output characteristics tend to deviate substantially as well as an increased risk of damaging the laser diodes. Cooks paper [7] provides relevant information relating to these effects, looking at Figure 2.5 and Figure 2.6 examples of temperature effects on LDs with respect to wavelength and current Vs power are shown. As temperatures rise in the semiconductors more energy is introduced in the p-n junction consequently creating a higher drift current all the while maintaining a stable voltage, also deduced from Figure 2.6 is as temperature rises the emitted photon wavelength will also increase to a different wavelength. To

achieve accurate and good quality output characteristics it is evident that heat management is another key element in LD operation.

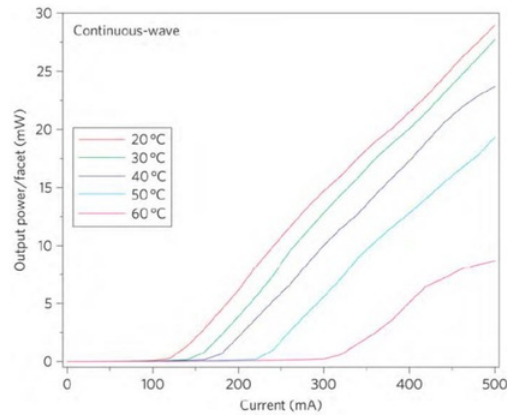


Figure 2.5: An example of how temperature effects current Vs output power[7]

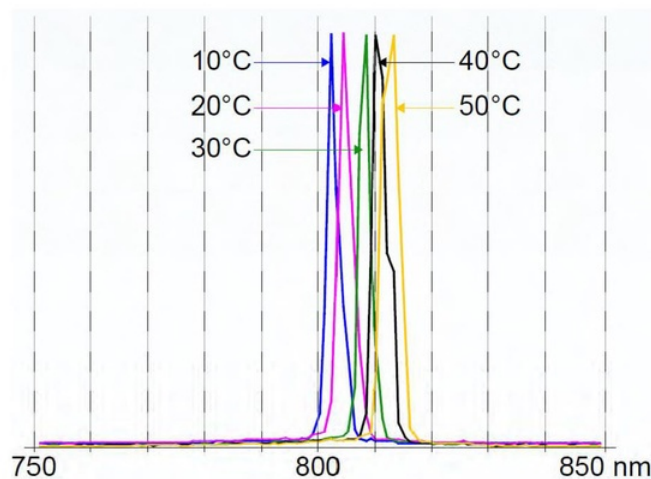


Figure 2.6: Example of LD temperature on emission wavelengths. [12]

2.4.2 Heat sinking

A common method used to help disperse heat in many electronic circuits is to attach an appropriately sized heat sink to the component that is creating the waste heat. The heat sink acts as a heat exchanger which transfers the waste heat created by any electrical or mechanical

component mounted on it to facilitate in dissipating the thermal energy from that component, this helps maintain a steady operating temperature the device requires. According to Hosung Lee [13] for any standard heat sink its performance is improved by increasing either "the thermal conductivity of the fins, surface area of the fins, or heat transfer coefficient". Hosung talks about how having fins in the heat sink greatly improves heat transfer and cooling effectiveness, as well as increasing once again overall surface area of the heat sink device. The most common heat sinks are made from copper or aluminium, it is said that even though copper has higher heat transfer rating aluminium has the better heat dissipation properties and is the reason why finned heat sinks are usually seen as aluminium. Calculating the correct size for each heat sink with respect to the heat it has to dissipate is the tricky part. Due to some materials used not specifying thermal properties a soundly proven technique was used to estimate the approximate heat sink volume needed for each diode. This technique was taken from articles [14] [15] [16] [17] which can be surmised that: volume of a heat sink under low conditions can be obtained by dividing volumetric thermal resistance with the required thermal resistance. Derived from basic thermal circuit equations we get:

$$(5) \quad V = \frac{Q * Rv}{\Delta T}$$

$V = \text{Heat sink volume}$

$Q = \text{heat source power}$

$Rv = \text{Volumetric thermal resistance}$

$\Delta T = \text{Max temp at junction} - \text{maximum ambient temp}$

Which gives an equation to calculate heat sink volume based on outside dimensions, furthermore Rv or 'volumetric thermal resistance' is based on a chosen value from Table 2.1 below.

Air flow (m/s)	Rv ($cm^3 \cdot ^\circ C/W$)
Natural Convection	500-800
1 (gentle)	150-250

2.5 (moderate)	80-150
5 (high)	40-80

Table 2.1: Approximate ranges of volumetric thermal resistance of a typical heat sink under different flow conditions

Given the LPC-840 maximum operating conditions being 2.2 volts at 340mA and the NDG7475 being 4.6 volts at 1.8A, we can calculate the photon and phonon produced by each diode.

$$(6) \quad \text{Power} = \text{Volts} * \text{Current}$$

$$P_{max_{LPC}} = 2.2 * 0.34 = 0.748 \text{ Watts}$$

$$P_{max_{NDG}} = 4.6 * 1.8 = 8.28 \text{ Watts}$$

As we know efficiency is the ratio of the emitted optical power to the applied electrical power as seen by equation (4), also referring to the datasheets for the LDs [LPC-840] [NDG7475] we can verify expected output power, using this we calculate efficiency:

$$\eta_{LPC} = \frac{0.5}{0.748} W = 0.66 = 66\%$$

$$\eta_{NDG} = \frac{1}{8.28} W = 0.16 = 16\%$$

Using these power conversion efficiencies this gives maximum ratings at:

$$0.66 * 0.748 = 0.493W \text{ emitted as photon and } 0.255W \text{ as phonon for the LPC}$$

$$0.16 * 8.28 = 1.32W \text{ emitted as photon and } 6.96W \text{ as phonon for the NDG}$$

From these values we use equation (5) to calculate the approximate heat sink volume required to effectively manage the heat of each diode. Selecting a volumetric thermal resistance (Rv) of 100 due to moderate to high air flow being provided and plugging in the values obtained we get:

$$V_{LPC} = \frac{\sim 0.3W * 100}{75^{\circ}C - 35^{\circ}C} = 0.8cm^3$$

$$V_{NDG} = \frac{\sim 7W * 100}{50 - 35} = 46.7cm^3$$

It should also be noted that maximum operating temperature of LD case was obtained from the data sheets [LPC-840] and [NDG7475]. With these calculated volumes the selection of a suitable heat sink module for each diode can be established. In this case heat sink modules with dimensions of 30*30*50 mm or a volume of 45cm³ were obtained; the heat sink value calculated for the NDG7475 was outside this range therefore additional cooling methods are going to be implemented for the diode.

2.4.3 Thermo-electric air cooling system

Thermo-electric coolers (TECs), also referred to as Peltier plates are solid-state heat pumps that incorporate the Peltier effect to move heat [18]. Usually featuring two different semiconductors, an n-type and a p-type, they are positioned thermally in parallel and joined at one end by a conducting cooling plate. The conducting plate usually made from copper or aluminium is used for the conducting of the different temperatures caused by the Peltier effect. According to [18] the Peltier effect is when a direct current is passed through a pair of dissimilar metals, the junctions, depending on material combination, tend to heat at one end and cool at the other, Figure 2.7 depicts how this actually occurs.

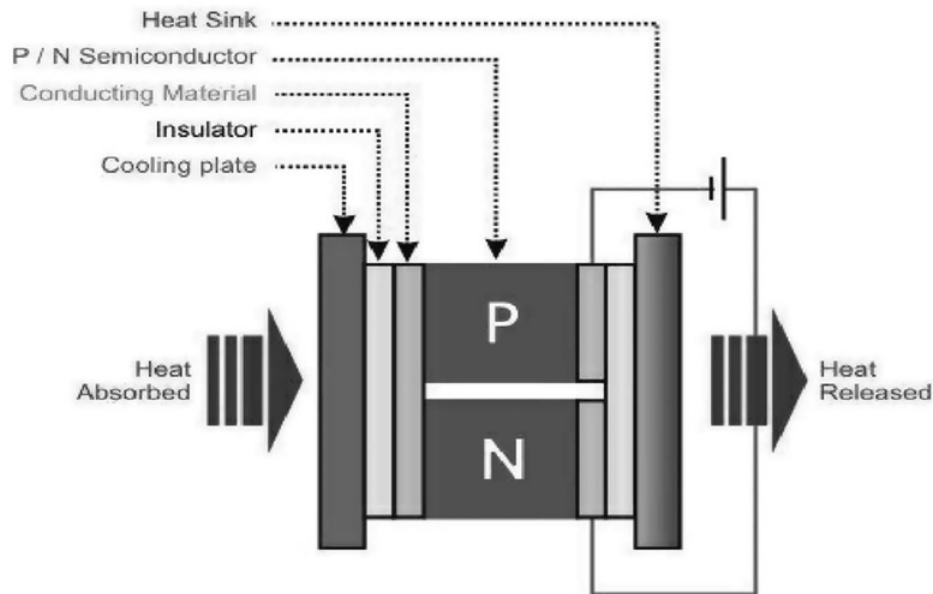


Figure 2.7: TEC system breakdown

When a DC current is injected in the junction of the semiconductors wired in series, a temperature change occurs between the two elements. Simply put, the voltage drop across the module draws the charge carriers in the p and n type materials down to the hot side, this is because thermal energy is encouraged to the hot side of the plate. This therefore brings energy away from the cold side of the plate reducing the temperature until the change in electrostatic potential brings the value of something called the Fermi levels of the semiconductors to equal levels.

Chang, Chen and Ke [19] have developed a thermal analogy model which analyses the thermal performance of thermoelectric air-cooling modules. The thermal analogy model can be seen in fig .. and can be directly related to electronic circuit analogy models, key points taken from their paper includes how effectiveness of the TEAC system is significantly affected by the temperatures of the hot and cold sides of the Peltier plate itself. It is critical to remove heat created by the hot side of the plate using some sort of heat dispersion method, preferably an air cooled aluminium or copper heat sink to keep heat build up to a minimum. In the project a thermoelectric air-cooling system will be glued to the underside of a heat sink module, the heat sink module will also incorporate a fan and temperature control module which will switch on and off to maintain the optimal LD operating temperature.

2.5 Laser beam combining technique

Laser combination in electrical-optical systems to this day prove to be quite advantageous especially in the pursuit of high power laser systems that require high beam quality. The general goal of beam combining is to not only increase the output power, but also preserve the beam quality, so that the brightness and intensity is increased just as much as the output power.

There are two main categories of beam combining.

2.5.1 Coherent beam combination

Coherent beam combining works with beams which are mutually coherent. techniques include (Coherent polarization beam combining, side-by-side combining and filled-aperture combining.)

2.5.2 Spectral beam combination

Spectral beam combining does not require mutual coherence, but rather uses emitters with non-overlapping wavelengths. The single beams are then fed into a wavelength-sensitive beam combiner, such as a prism, a diffraction grating, a dichromatic beam splitter (dichroic mirror), or a volume Bragg grating [20] [21]. The input beams that have been sent through the other side of the wavelength-sensitive beam combiner now appear in a single beam, where the input beams have been made co-linear.

In regards to intensity and efficiency both SBC and CBC will provide near-diffraction-limited output and equivalent brightness according to [22] .

In the project we use a dichroic mirror to combine the beams, which is one of the most commonly encountered optical component used for beam combination. The technique has been used for years in the enabling of beams with different wavelengths to be combined with increased efficiency and intensity, an example of how this works can be seen in Figure 2.8 [22] With respect to the project a red pass, green reflect type of mirror will be utilized which will reflect the emitted green visible light and allow the emitted red visible light to pass through the prism.

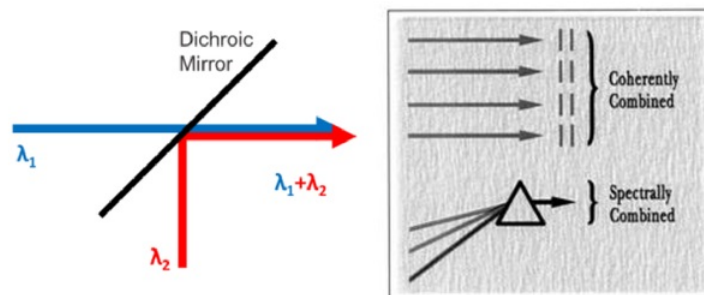


Figure 2.8: Dichroic mirror (left), Coherent and Spectral beam combining (right)

2.6 Optical Alignment [25]

With respect to any kind of photonics, optical alignment is the most important factor in achieving a stable and efficient output. For example the task of aligning the collimated light from a single laser diode into an optical fibre requires the fibres end to be within fractions of a millimetre of the lens' focussing point otherwise it can lead to some form of undesired divergence of convergence. The optic fibre being coupled has a core diameter usually varying in the microns, the core being at the fibre end also should have undergone the correct cleaving procedures to produce a clean and close to perfect cut. Having to align the collimated light from the LD to the centre of the focussing lens and then that light into the fibre's end is quite a complex procedure. Improper alignment usually leads to some sort of power loss due to some portion of light not being sent through the fibres core, fire and safety hazards can also arise due to errant beams. For most optical component alignment procedures there are 6 typical degrees of freedom to work with. With relation to the most common axes there are the 3 translational axes also known as x, y, and z. The other three axes relate to the three rotational axes, it should also be noted that the two sets of axes are not independent of one another. For example, the collimated light of a LD might be in the correct target position but be at the wrong angle. Any action taken to correct this would require a rotational adjustment which would move the beam off the target point, this would then require some further translational adjustment. What also must be considered is the effect of multiple components being aligned and their interactions. If for example one component were to be properly aligned a second component may have to be realigned to properly match the first components axes. Take a focusing lens and a fibre optic aligner for example, If the focusing lens were to be moved the component aligning the fibre ends core with the focus point of the focusing lens will also have to be re aligned, this could also lead to a cascade of adjustments through the electro-optical system.



Figure 2. 9: Optical breadboard/Table used to support systems used for laser and optics related experiments, engineering and manufacturing.



Figure 2. 10: LineTool.co ALH 3 axis linear translation stage device used for precision alignment which includes M3 threaded holes for bracket systems.



Figure 2. 11: XYZ 3 Stage - course/fine Fibre Aligner

There are numerous ways to properly align optical components, however the most common and stable process is to use an optical breadboard or table which can be seen in Figure 2. 9. The optical breadboard provides a flat rigid surface that gives high degree of accuracy for components bolted onto it. The breadboard provides M6 threaded holes with a standard pitch of 25mm which corresponds to the standard hole size optical components usually conform to for mounting. In regards to fine positioning of certain components in the translational axes a Line Tool ALH 3-axis linear translational stage device was used which can be seen in Figure 2. 10. The device as its name suggests can perform course adjustments independently in each of the axes. As for the rotational axis adjustments in this case no optical components require rotation as part of its operation so it will not be used. Finally for the precise alignment of the fibre independently of the other components a linear motion stage fibre aligner was used which could perform course and fine adjustments to the micron in the X,Y and Z axes independently of one another which is crucial in fibre coupling as mentioned previously, the component is depicted in Figure 2. 11.

2.7 Stimulated emissions in medium

Referring to the two papers [7] and [23] , the concept behind stimulated emission in fibres is explained. Similarly to what was explained in the electro-luminescence process, the process of stimulated emission in optic fibre has a parallel concept. First what should be acknowledged is the process behind particular atoms moving from a 'ground' and 'excited' state. As it's known atoms are made up of electrons orbiting a nucleus, the electrons would normally sit in a low orbit called the 'ground state'. If provided enough energy the electron in that low orbit could absorb some of that energy and would be able to sit in a higher orbit called the 'excited state'. This is the process that occurs when an electron moves from a lower orbit to a higher orbit. Furthermore if an electron was already in its excited state and wanted to return to its ground state or some lower state a process called 'decay' occurs, which is the same process that occurs in the electron-hole recombination concept. Basically the electron must lose energy to reach the lower orbit and this often happens by releasing energy and emitting light. If the electron trying to get to an excited case does not receive the correct amount of energy from a passing photon, nothing will happen;

this usually occurs due to different materials require different amounts of energy to achieve that excited state.

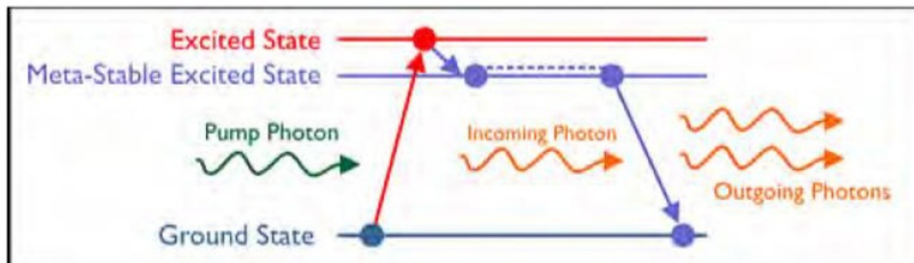


Figure 2.12: Stimulated emission in doped fibre

Looking at Figure 2.12 the transition of the electrons state can be seen. The pump photon provides the energy needed for the transitioning process to begin. The key in this case stated by Cook [7] is that the decay from the excited to ground state is triggered by somewhat coherent light and hence produces a steady output in the decay photon emissions. In most fibre laser systems, a 'optical cavity' is usually introduced to enhance the gain in the fibre, the process usually involves reflecting the photons back and forth through the fibre causing a cascade of photon stimulation. In the case of doped fibre systems, a specific pump source wavelength will be required to stimulate the transition of electrons to their respective excited states and hence cause a decay process which will allow the electrons to reach a specific meta-stable excited state as seen in Figure 2.12. This state usually is equivalent to an emission wavelength different (in most cases longer) than the pump wavelength introduced in the system i.e. pump giving visible infrared, and producing mid infrared waves at the output. Looking at the partial energy diagram in Table 2.2 the different levels of infrared laser emissions can be seen from holmium ZBLAN fibre. These different emission wavelengths give speculation on what can be expected for the end project and the wavelengths that may result.



transitions in red [23].

2.7.1 Superluminescence

A phenomenon which sometimes occurs in fibre laser systems is superluminescence. This process usually occurring in the laser system medium is the emission of luminescence that has experienced optical gain via stimulated emission. Due to the finite gain bandwidth, the bandwidth of the emitted light is usually smaller than that of the luminescence itself. Superluminescence is often used for generating light with a broad bandwidth and one of the main experimental questions in this project is if the laser system designed will in fact produce some form of broadband infrared signal from the doped fibre being used. [24]

3 SYSTEM MODEL AND DEVELOPMENT

A diagram of the overall system is shown in Figure 3.1, we can see the two laser diodes incorporated in their heat management systems as one item. To combine the light one dichroic mirror will be used, the dichroic mirror will have the properties that will allow the 660nm red light to pass through one side of the mirror and reflect any 520nm green light from the other side.

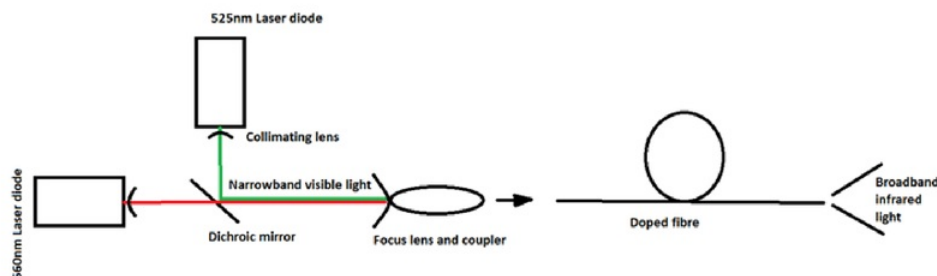


Figure 3.1: Schematic diagram of laser combiner system

The mirror will be aligned and angled as close to 45°C as possible to achieve co-linear beam paths, once combined light is achieved it will be sent through the implemented fibre coupling system with some fibre optic cable attached. The measurement of how much light getting into the fibre will then be performed and optimization methods executed to achieve maximum light in the fibre. To measure the light going into the fibre, combined power of the lasers will be measured and compared to the fibre optic output power, the difference will tell us how much

light we are essentially losing. Once optimization methods have been completed a doped fibre optic cable will be used in the system where the power and wavelengths will also be analyzed.

3.1 LPC-840 improvised components

Due to parts still not having arrived from international locations, the suggestion of building a cheap current limiter circuit from salvaged electronic components was utilized to test the output capacity of the LPC-840 as the actual datasheet for the LPC-840 was not entirely provided and online sources seemed not to be 100% reliable. Referring to datasheet [LM317] we see a basic current limiter circuit which is a given circuit provided by the LM317 datasheet, modifying the circuit as seen in

Figure 3.2 to allow for adjustable current and laser diode protection is shown.

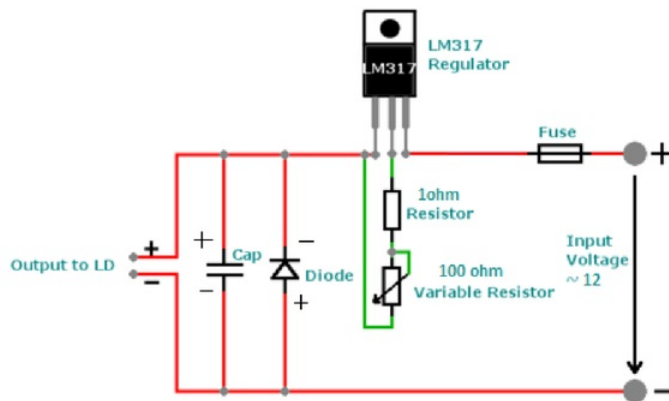


Figure 3.2: Wiring diagram of Current Limiter Circuit

The components incorporate a LM317 voltage regulator IC with a mounted heat sink, 1 amp fuse, 1Ω resistor, 100 Ω potentiometer, a single 1n54004 rectifier diode capable of 3 amps and a reverse peak voltage of 400 volts, a 10µF capacitor with a voltage rating of 63 volts and basic wiring sundries. The capacitor was added to protect the diode from any voltage spikes that may occur as the diodes are very sensitive and will only operate in a voltage range of approximately 2.2-3 volts. It should be noted to ensure the capacitor is connected the correct way, where the negative side is connected to the negative power supply cable and the negative laser diode cable in parallel. If connected incorrectly any charge in the capacitor that has accumulated may be forced in the laser diode all at once and destroy it. Furthermore the 1n54004 rectifier diode is placed in parallel to the capacitor with opposite terminals connected to each other. This rectifier diode protects the laser diode from any reverse voltage or current that may occur from accidental reverse wire connection, once again the laser diode is very sensitive and can only handle around 80mA of reverse current or 2V of reverse voltage before it is damaged or ruined. The rectifier

diode chosen can handle approximately 400V, 1A of reverse conditions before allowing anything to go wrong, which is well over the limits we are supplying; the complete circuit can be seen in Figure 3.3.

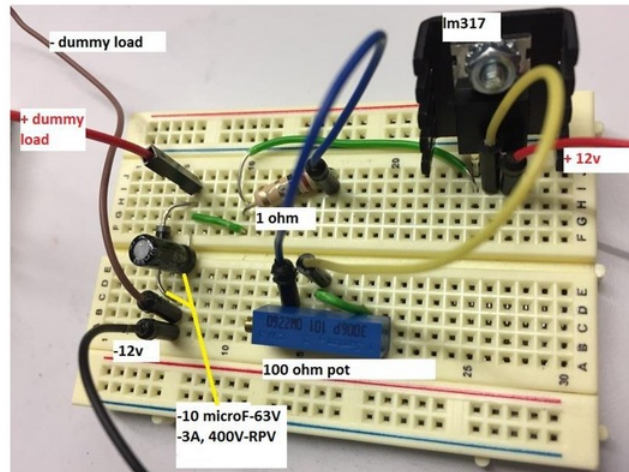


Figure 3.3: LM317 Limiter Circuit

3.2 Driver Calibration

A common precaution taken before connecting laser diodes to unused and in this case cheap drivers is to build a circuit that will act as a test load. This means the circuit acting as the test load should be built to act as the laser diode chosen. Using simple 1n54004 rectifier diodes and 1 Ω resistors are enough to build the circuit in question.

3.2.1 LPC-840 dummy load

Referring to the datasheet [LPC-840] the LPC-840's operating voltage is anywhere between 2.35-3 volts, this means we need to select a certain amount of rectifier diodes which when combined will have a voltage drop of anywhere in between the operating voltage stated. It should also be noted as introduced amperage becomes larger the voltage drop over the 1 Ω resistor will also increase, keeping this in mind the voltage drop across all the rectifier diodes and resistor should equal that to the operating voltage of the laser diode. The current in this case will be a maximum of 500mA, which will equal a maximum voltage drop of 500mV over the resistor. Choosing 3 rectifier diodes and where the voltage drop of each of the diodes equal to $\sim 700\text{mV}$ and wiring them in series will suffice.

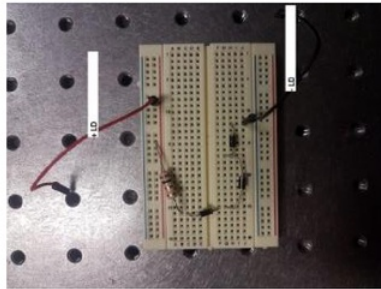


Figure 3.4: LPC-840 dummy load

3.2.2 NDG7475 dummy load

As mentioned before the test load has to be configured according to the laser diodes specifications. Referring to data sheet [NDG7475] we see the operating voltage of the device is around 4.6 volts. Using 6A10 rectifier diodes and a 5 watt capable $1\ \Omega$ resistor as precaution (due to more current being introduced in the circuit) the circuit can now be constructed.

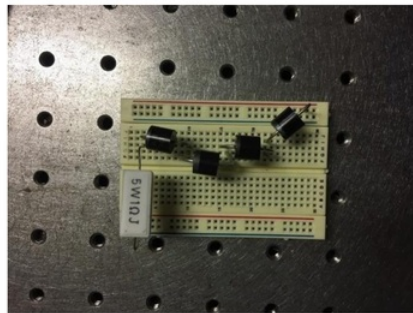


Figure 3. 5: NDG7475 dummy load

In Figure 3. 5 we see 5 x rectifier diodes in series with the $1\ \Omega$ resistor, the voltage drop across the diodes will equal around 3.5 volts, with an expected current of 1.2 amps that will add up to approximately 4.6 volts across the circuit. If one were to increase the current supplied to the diode, adjustments would have to be made to the rectifier diodes accordingly to produce the specified voltage drop the diode would have. Once the test load is connected to the driver circuit, measurement over the $1\ \Omega$ resistor was done while adjusting the potentiometer to set the specified driver circuit current before initial diode testing was done.

3.2.3 LPC-840 improvised heat sink

Since the heat sink being shipped had not arrived a improvised heat sink was built for diode testing procedures. Looking at data sheet [LPC-840] we can see the diameter of the outside ring of the diode is $\sim 5.6\text{mm}$, a hole this size was then drilled into a piece of salvaged aluminium and the diode placed inside. Looking at Figure 3.6 we can see the driver and diode attached with the heat sink. Thermal compound was also used to eliminate any air gaps between the diode and heat sink for optimal heat transfer.

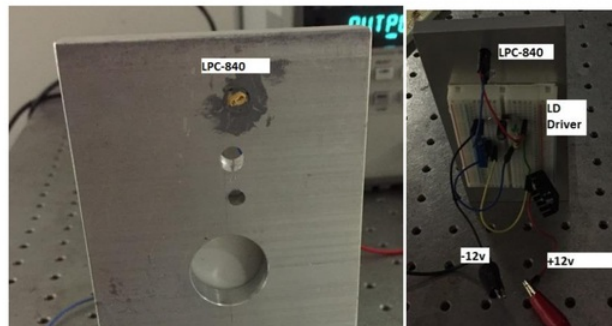


Figure 3.6: (left) Heat sink with diode, (right) Diode in heat sink, driver and power supply connected

3.3 Component Testing, Calibration and Connections

Once components started arriving, testing of their performance characteristics were carried out and compared to the given characteristics. Due to parts being low-cost these tests were conducted to observe how accurate the specifications were and how much the components could actually tolerate; components connected in the system and their preferable settings used in the project are also mentioned. Each laser driver was first tested for their maximum current ratings, this was done as previously mentioned by connecting a dummy load to the driver in place of the LD and measuring how much current was going through the resistor while adjusting the variable resistor on the driver.

3.3.1 Component Testing

For the [DB650-50-500-12V-BL-LM] driver the maximum current allowable was recorded to be 220mA. That is almost 300mA less than specified, keeping in mind however these parts are cheap and it was presumed that the hardware operating characteristics were going to be lower

than specified. In addition the [12V-150-500-LD] non-adjustable driver produced a maximum current of around 170mA. Furthermore the [5V-200-800-GD-RD] 0-200mA red LD output and 0-800mA green LD output driver produced a maximum current of 200mA for the adjustable red LD output and a maximum of 500mA for the adjustable green LD output. In addition the [DB-12V-200-3500-GD-LM] adjustable driver was tested similarly, this driver is used in conjunction with the NDG7475 diode, measurements determined maximum current for the driver is 2.8 amps. Finally the SXD-v3 2.4A driver was tested with a dummy load, maximum current rating for the driver was measured to be up to 3.1 amps at 12 volts, however the driver current can only be adjusted by regulating the input voltage. The Peltier cooling plate [TEC1-12706 COOLING PLATE] provided a current draw of 4 amps at 12 volts which is 2 less amps than stated at 12 volts. Understandably most components were lower than their specified ratings, however the components selected are adequate for the desired performance for their respective laser diodes.

The laser modules used include a 30x30x50 mm heat sink that has a 12mm diameter thread for a T0-18 & T0-5 diode host/housing, the host includes a glass coated short focal length adjustable lens for collimating the diverged output of the diode. The module also includes a small 12 volt fan for direct ventilation and cooling of the mounted laser diode. Looking at Figure 3. 7 we see the module and driver connected with some collimated light in the far field. The lens given seemed to have a short focus point, which occurs only centimetres away from the front of the lens itself. A 3-element, aspherical, anti-reflective coated lens with an EFL of around 2.3mm was purchased for the LPC-840 module, the lens has been able to provide lower diverging output at further distances, this decreased divergence will help with maintaining a higher power output for the diode at further distances if need be.

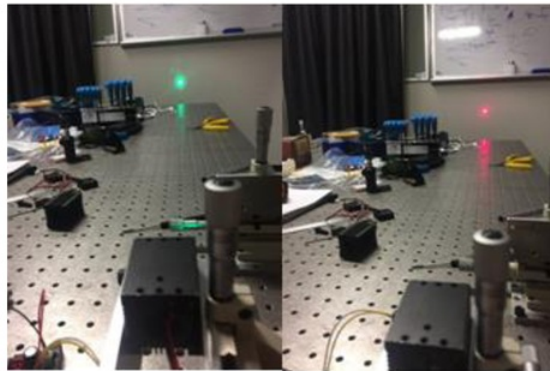


Figure 3. 7: Collimated NDG7475 (left), LPC-840 (right)

3.3.2 Components Utilized

Once the actual component specifications were realised and maximum capacity tests were conducted with various components in connection the following components were chosen and set with the following parameters to provide optimal performance while the system was active:

- For the LPC-840 diode driver, the [5V-200-800-GD-RD] driver was used and set to maximum (which peaked at around 450mA for a maximum current limit), the driver was run at 6 volts, it was noted the driver is specified for 5 volts however this would allow more current to the diode and no temperature increases were noticed over the circuit board and its components.
- The NDG driver used was the [DB-12V-200-3500-GD-LM], since anything over 2 amps would cause the TEC module to be redundant and power loss started occurring at that specified current the driver was set to 2 amps for optimum power output.
- The TEC plate [TEC1-12706 COOLING PLATE] was used in conjunction with a DC-DC step down regulator [LM2596 STEP DOWN REGULATOR], this step down regulator was set to 10 volts as anything over 10 volts would draw too much current from the TEC plate and with the heat sink provided, could not sufficiently transfer the heat the TEC plates hot side was creating, thus causing an overflow of heat to the cool side of the TEC plate and offer no cooling behaviour.

The components mentioned were connected to a power supply, although these components were the main driving elements of the system there were a few other essential components used which can be seen in Figure 3.8, which includes a diagram of all components connected together and their corresponding settings. It should be noted that the TEC module and the NDG7475 are glued together however for an easier understanding of component relationship they are not shown together in the diagram.

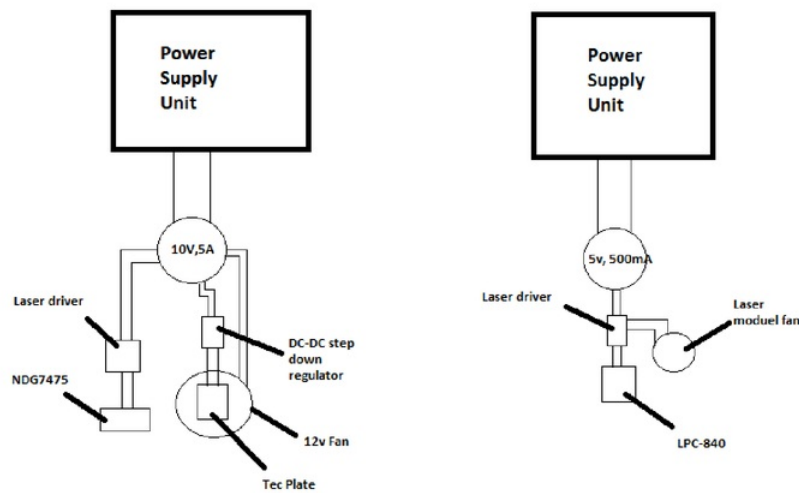


Figure 3.8: Basic wiring diagram

3.4 Laser Diode Testing

3.4.1 LPC-840 Distance Test

Measurement of output power produced by the diode over different current settings and at a distance of 500mm was then recorded. The distance referring to the length between the diode output facet and the power meter measuring device. Referring to Figure 3.9 the loss in power over the distance selected is obvious and was expected, with the help of a lens the diode can maintain a power output of above 200mW at around 400mA. Comparing this to the measured results using the old lens, there was an increase of around 100mW when running the diode at 400mA.

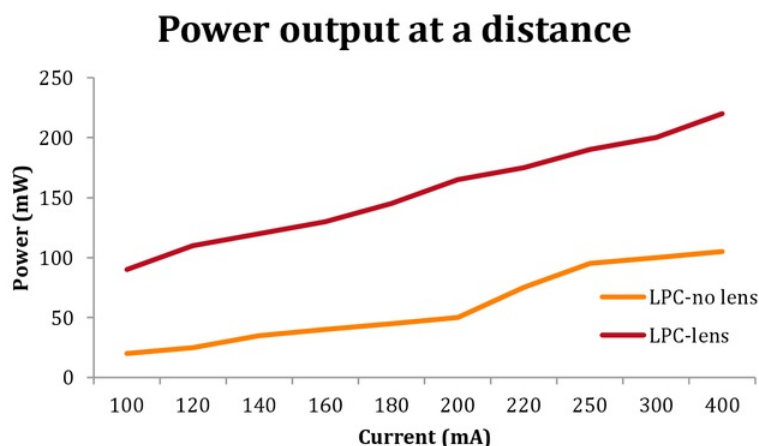


Figure 3.9: Power and current relationship for the LPC-840 with and without a lens at a distance of 500mm

3.4.2 LPC-840 Close Range Test

Next the LPC-840's power output was tested as close as possible to the thermal power meter measuring device, this test was done with the same current settings however the distance between the diode output facet and the power meter were aligned flush. The results were then compared to the previous test results of the diode at a distance. Looking at Figure 3.10 we see the difference in power output the laser has immediately, the diode without a lens can produce a maximum of 480mW at 400mA at the point closest to the light is being produced, however this was pushing the diode well above its maximum rating and is not advised to use the diode like this for continuous use as it will diminish life expectancy substantially. Comparing to the power output with a lens we see the power seems to stop increasing between 200-400mA, this loss was expected and was deduced to be caused by light lost from passing through the low-cost lens. Looking back at Figure 3.9 and comparing to Figure 3.10 we can see the effect the lens has on the device at a distance where it is able to maintain a maximum power output of up to 220mW with a lens, where as compared to the device with no lens the divergence caused an effect which would only allow a maximum power output of around 100mW at that distance and with the same current supplied.

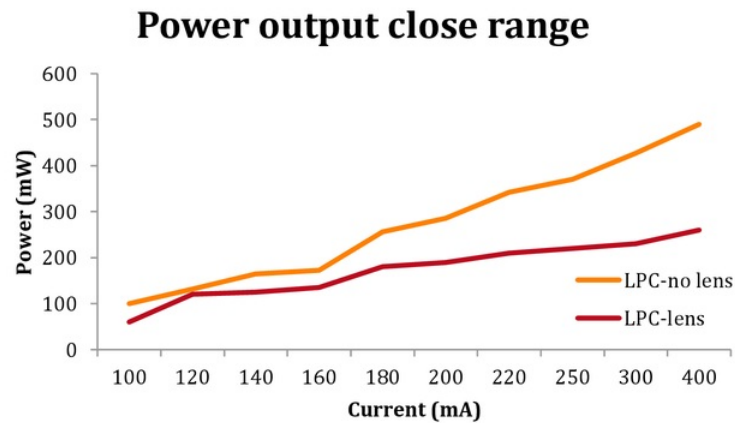


Figure 3.10: Power and current relationship for the LPC-840 with and without a lens

3.4.3 NDG7475 Close Range Test

Testing the NDG7475 diode was then performed at the same distances and using currents ranging from 1 amp to 2 amps. At close range it is evident that the diode performs as expected when comparing Figure 3.11 to the specified data sheet given [NDG7475], also we can see the diode can produce roughly 1.3 W at 2 amps, however without the proper cooling system the diode produces a large amount of phonon quickly and will cause a decrease in power as the diode keeps building heat. Furthermore looking at Figure 3.11 we see the maximum power output of the diode with a lens stops at 1 W, this loss again is expected and is due to light loss from passing through optical components.

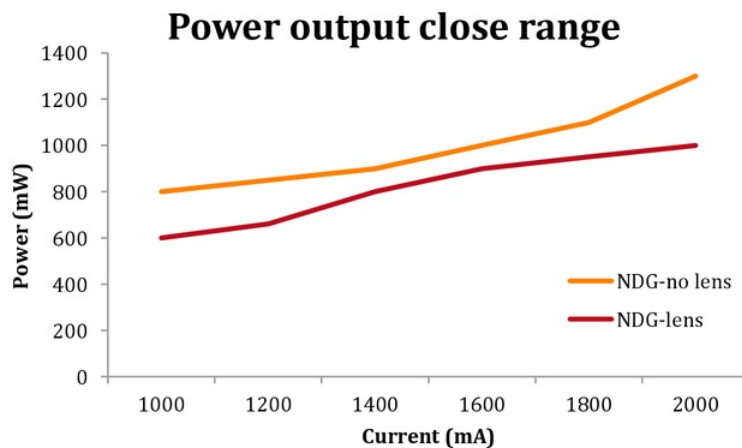


Figure 3.11: Power and current relationship for NDG7475 with and without a lens

3.4.4 NDG7475 Distance Test

Next the power output the NDG7475 could maintain over a distance was measured, looking at Figure 3.12 it is evident once again the effect a lens has over a distance. It should also be noted the distance is the same as the test with the LPC-840 that being 500mm. Looking at max power the diode can maintain with a lens it shows roughly 800mW, comparing to the power the diode is producing right at the output, a loss of 200mW is calculated. Considering the distance and the low-cost components the power loss is considerable, however will suffice for experimentation.

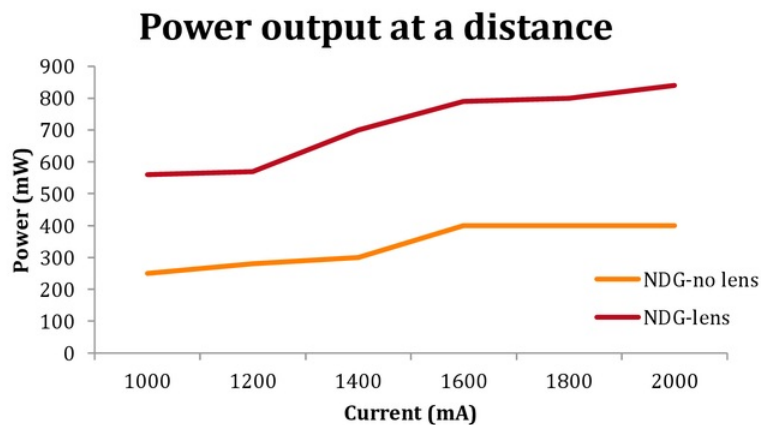


Figure 3.12: Power and current relationship for the NDG7475 with and without a lens at a distance of 500mm

3.4.5 Beam Divergence and Collimation Testing

Next the measurement of beam divergence over different distances while passing through a collimation lens was recorded. This was done by mounting the diode module on the optical table and setting up a sheet of paper at different distances to the diode while measuring the diameter of the beam that was observed. The lenses were also adjusted to focus at a point at the furthest distance which would provide the closest unchanged and non-diverging beam diameter when measured at these different distances. At a distance of approximately 1 meter and then 300mm the diameter of the collimated light of the LPC-840 was measured to be 4mm with the current lens and 3mm for the NDG7475 and its lens. It is important to ensure the beams of both lasers are in fact collimated as once this collimated light passes through the focussing lens it will ensure optimal results for fibre coupling.

A simple procedure was used to test if collimation was achieved for both diodes; two apertures were aligned in front of the diode being tested, one further back from the first at the same height. Once the laser was emitting light and going through both apertures one was moved closer and then further away from the other aperture while maintaining a position directly behind the first. If collimation was unsuccessful any non-linear light should appear on the iris of the aperture and indicate in which direction, lens or component adjustments are needed. It is important to achieve correct collimation for both diodes, if there is any light diverging, converging or aligned at an incorrect angle, the light trying to be put into the fibre will show significant loss.

3.5 Optical Alignment Procedures

With the gathered specifications on each component the optics experiment involving the combination of the visible diode light and sending it through some fibre can commence. Adding a simple TEC system with fan cooling to the NDG7475 module and thermally gluing all components together for optimal heat transfer the diode modules can be mounted to the 3 axis translational stage component. The TEC system incorporates a [TEC1-12706 COOLING PLATE] Peltier plate where the cold side is glued to the laser module flat surface and the hot side to a fan cooled heat sink salvaged from a computers CPU. Keep in mind a bracket system was made up by METS at the university to properly secure the diode modules in place for accuracy. It is crucial to align the two diodes similarly to that seen in Figure 3.1, next a mirror holder incorporated into a stand was used and bolted on the optical table with the reflective side facing the NDG diode and the pass side facing the LPC diode. The procedure required multiple attempts to properly angle the mirror as close as possible to ensure the beams were co-linear, as well as getting the height correct with the beam hitting preferably the centre of the mirror for each diode. Next a focussing lens mount attached to another 3 axis translational stage device is bolted to the optical table in the oncoming path of the combined beams; the goal is to get a position as close as possible so the combined light of both diodes hits the centre of the focussing lens. A tip would be to set up the fibre optic aligner first as it is the goal target position of the light and in doing this you would not have to re-position mounts to ensure the lights direction is going in the correct location. You should ensure the focussing lens is set up millimetres away from the fibre optic aligner, as the focus point of the focussing lens is quite short and minimal light loss is crucial on this part. The setup optic system can be seen in Figure 3.13 which includes component labelling.

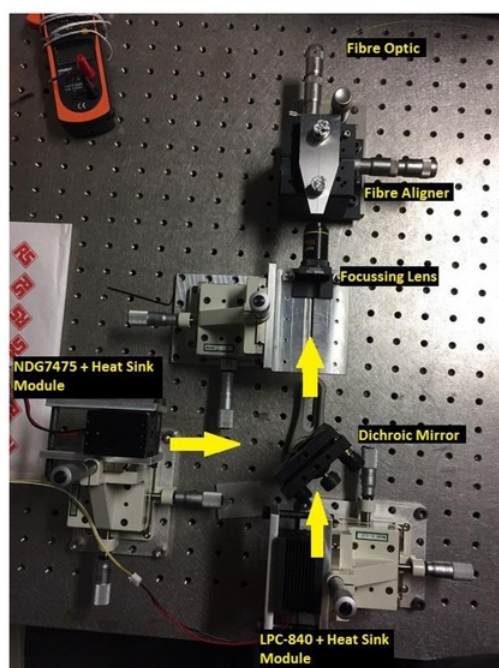


Figure 3.13: Aligned electro-optical system with labelled components

Once all optical components were mounted to the table, adjustments were made on each aligning tool while the lasers were active to try ensure the collimated beams of light were not only co-linear but also coaxial, while the lasers were active the beams direction can be observed and gives an understanding of the bearing the laser beam needs to be adjusted to. Once the lasers and the optical components were aligned to be coaxial by eye, optimal alignment procedures were undertaken; Figure 3.14 shows the two beams collimated and aligned on the same axes.

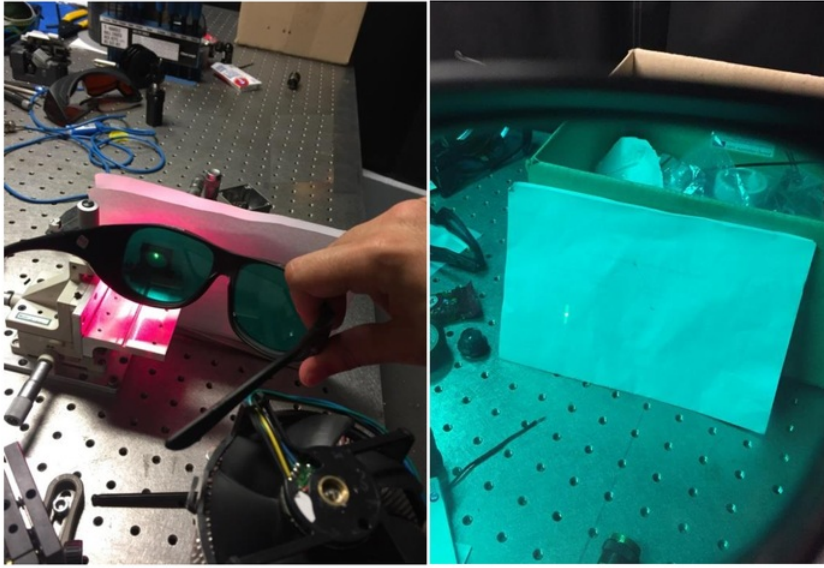


Figure 3.14: Coaxial beams near (Left), Coaxial beams far (Right)

3.5.1 Focussing Lens Efficiency Tests

Next, tests were conducted on multiple focussing lenses to give a broad idea of what power could be expected as light is passed through the dichroic mirror and exits the corresponding focussing lens as mentioned in table 3.1. The diode drivers were set to their recommended current settings as maximum drive was not necessary for this procedure. The NDG running at 1.5 amps gave a output power of 500mW and the LPC at 200mA gave a power output of 165mW, together they provided a combined power of 600mW; the following results can be seen in Table 3. 1.

Lens	Optical components	Efficiency (mW)
Green Coat – 10/0.25	LPC + Dichroic Mirror + Focussing Lens	$\frac{144}{165} = 87.3\%$
	NDG + DM + FL	$\frac{400}{500} = 80\%$
	NDG + LPC + DM + FL	$\frac{500}{600} = 83.3\%$
	LPC + DM + FL	$\frac{131}{165} = 79\%$

Blue Coat – 10/0.25	NDG + DM + FL	$\frac{325}{500} = 65\%$
	NDG + LPC + DM + FL	$\frac{430}{600} = 71.7\%$
Green Coat – 25/0.50	LPC + DM + FL	$\frac{150}{165} = 90.9\%$
	NDG + DM + FL	$\frac{400}{500} = 80\%$
	NDG + LPC + DM + FL	$\frac{505}{600} = 84.1\%$
Red + Blue Coat - FL10B	LPC + DM + FL	$\frac{135}{165} = 81.8\%$
	NDG + DM + FL	$\frac{20}{500} = 4\%$
	NDG + LPC + DM + FL	$\frac{140}{600} = 23.3\%$

Table 3. 1: Focussing Lens efficiencies

Looking at Table 3. 1 under the optical components column we see what laser and the components the light is travelling through, for example LPC + DM + FL provides an efficiency for the LPC diode active on its own as it passes through the dichroic mirror and the corresponding focussing lens as mentioned under the lens column. It should be noted the LPC and NDG terms include their laser module collimating lenses. The efficiency tests were achieved by measuring the power output of the light as it passes through the dichroic mirror which would act as Power in and dividing this by the power out measured from the focussing lens commonly known as the efficiency equation P_o/P_{in} . Evidently as seen in Table 3. 1 the green coated lens 25/0.50 has the highest efficiencies with some reaching up to 90% however due to the numerical aperture of the SMF-28 fibre we are using, this lens would cause too much light to be lost. Instead the green coated 10/0.25 lens will be used where it provides the second highest efficiency ratings on all parts. It can also be seen from Table 3. 1 the FL10B lens with the worst efficiencies that having less than 5% for the NDG diode light.

Testing for the maximum power through the green coated 10/0.25 lens was also performed just to ensure no problems were occurring at maximum running capabilities, running the NDG at 2 amps and the LPC at 400mW the combined power output recorded was 820mW through the mirror. Max power for both diodes as it passed through the focusing lens was 700mW giving an efficiency of 83.3%.

3.6 Fibre coupling

Once the light was successfully coupled in the fibre, power measurements were recorded for the laser diodes one at a time and together, which was then used to calculate launch efficiencies of the system. The launch efficiencies would help understand how much light was actually being lost in the system due to alignment or other optical related complications; in addition further calculations could also be made from these launch efficiencies to select an appropriate fibre which has been doped by some rare earth elements. With the selected fibre implemented in the electro-optical system, some form of superluminescent light may be seen as a result.

3.6.1 SMF-28

The single mode smf-28 fibre was used to calculate launch efficiencies of the system. The specifications of the fibre used can be seen here [Corning SMF-28], looking at the data sheet it tells us that the fibre has a core diameter of $8.2\ \mu\text{m}$ with a core cladding of $125\ \mu\text{m}$. Knowing this an appropriate focusing lens was selected out of the lenses provided to produce a focused point small enough that would allow the optimal amount of light to pass through the fibre once aligned correctly; in this case the 10/0.25 lens with the green coated lens layer was selected. The first step which sped up the alignment process in this case was to align the fibre in a position that would allow the most light in the fibre by observation, of course this could only be done with lasers producing light in the visible wavelength. Once most light could be seen going through the fibre optimal alignment measures were performed, which involved setting up a sensitive thermal power meter at the output end of the fibre and adjusting each axis on the fibre aligner until maximum power was achieved. A final step to ensure optimal power in the fibre was to adjust the dichroic mirror rotational alignments, this would only optimise how much light the green laser would get in the fibre without disrupting the other light source, this again was also performed with the power meter connected at the output of the fibre.

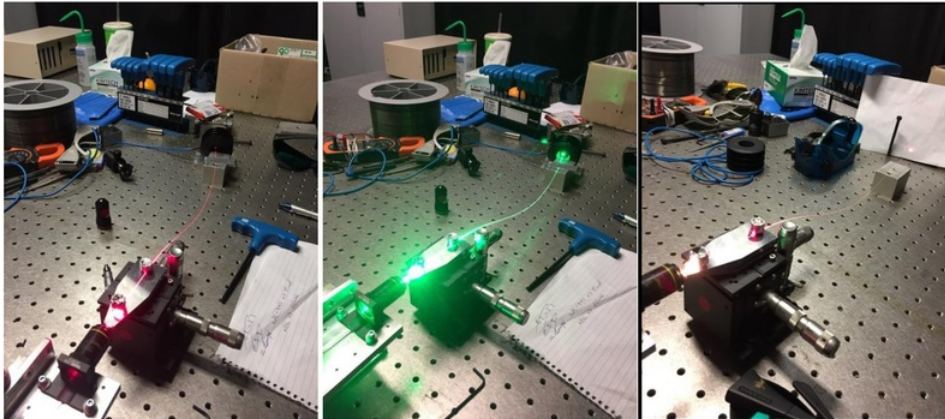


Figure 3.15: Red light in smf-28 (left), Green (middle), Combined (right)

	LPC (mW)	NDG (mW)	LPC+NDG
Launch Efficiency	$\frac{80}{165} = 48.84\%$	$\frac{30}{500} = 5\%$	$\frac{110}{600} = 18.3\%$
Overdriven LPC	$\frac{90}{165} = 54.54\%$	$\frac{30}{500} = 5\%$	$\frac{120}{600} = 20\%$

Table 3.2: Launch efficiencies of light into smf-28

Looking at Figure 3.15 the light going in the fibre with the red, green and then both sources turned on can be seen, efficiencies calculated for the diodes when running alone and together can also be seen in Table 3.2. Looking at the results calculated we see more than 45% of the LPC-840s light is being sent through the single mode fibre, it was speculated that this might be the case as the LPC-840 is a single mode laser as compared to the NDG7475 being a multimode laser. The NDG7475 alone shows only 5% of the power its producing is being sent through the fibre, which is quite low however still sufficient for the experiment. Finally with the beams being combined, a launch efficiency of 20% was calculated, this kind of experiment has not been done before with Bedrock Photonics so there was no speculation of what efficiencies should or could be expected.

3.6.2 Holmium doped ZBLAN fibre - 0.5m

From the SMF-28 launch efficiencies calculated a doped fibre with the suitable properties was selected, the fibres specifications can be seen [Holmium ZBLAN], we see the cladding diameter and core diameter are fairly close to that of the SMF-28's, so launch efficiencies should remain the same if not a small amount better. A 0.5m piece of Ho ZBLAN fibre was cut, cleaved and set up in the place of the SMF-28, the same alignment procedures were performed for maximum power at the fibres output. This included once again adjusting the 3 stage fibre aligner until the highest power reading was achieved, all other optical components have been already positioned from before and need not be touched. From this 35mW of 520nm Green light and 50mW of 660nm Red light was recorded at the output, together giving a total of 85mW of visible light.

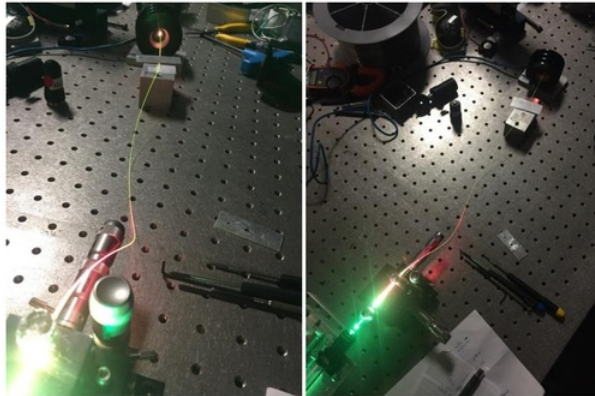


Figure 3.16: Combined light in Ho ZBLAN fibre with observable luminescence

Looking at Figure 3.16 the light being sent through the fibre while both pump sources are active can be seen, it is interesting to note the different colours that are being produced which tells that some light stimulation is in fact occurring in the doped fibre giving off different wavelengths. Next another optimization procedure was undertaken before the OSA was set up and the spectrum analyzed, this procedure was used to maximize absorption of the combined light in the fibre for optimal IR light emission. A single IR band-pass filter is mounted at the output end of the fibre, the specifications of the filter can be seen [FB3000-500

]. The filter was used in this case to block out all light that was not in the 2500 - 3500 nm wavelength range, next a photoconductor is set up as close as possible behind the filter, the photoconductor will be used to detect the MIR wavelengths the filter is allowing to pass through. The photoconductor (MIR detector) used is especially sensitive meaning the way the circuitry is designed is for minimal noise thus blocking out all DC inputs, this means it requires any optical input to be chopped.

Once all components were mounted to the optical table, alignment of the fibre for maximum absorption is performed, this is done the same way maximum power in the fibre is achieved. Results showed a combined input of 1.2mV or 1.2mW (being directly proportionate to power) of MIR being detected while both pump sources were active, alone the red was detected to have around 0.9mW of MIR light and the green 0.3mW. Finally the OSA was mounted at the output end of the fibre where a sweep was performed, emission readings around the 2850nm wavelength was detected which can be seen in Figure 3. 17

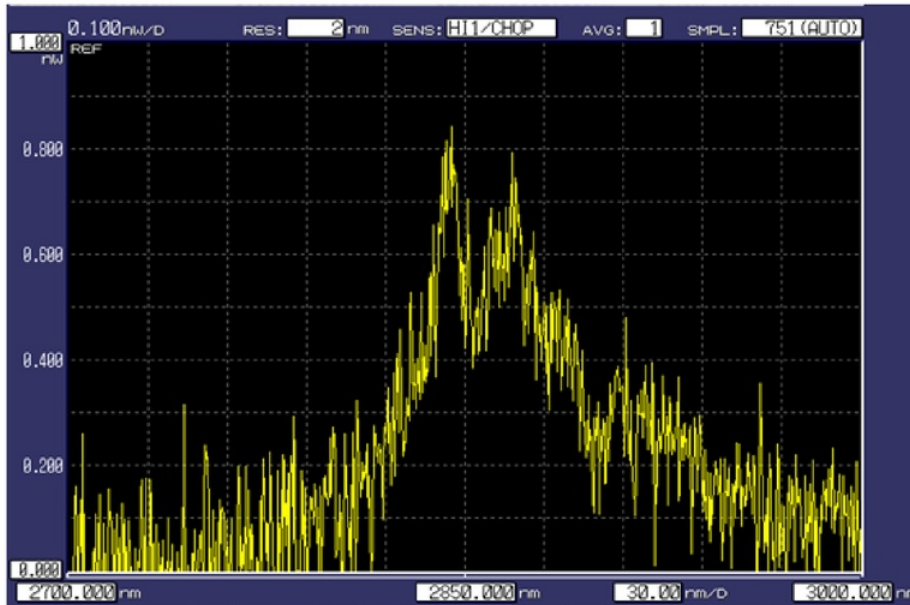


Figure 3. 17: OSA reading from 2700nm - 3000nm

The MIR emission seen around the 2870nm wavelength is important towards Bedrock Photonics research. A peak reading of around 800 pW is given, however small this proves some form of superluminescence is being achieved from the electro-optical system designed.

3.7 Single diode as pump source in Ho ZBLAN fibre

During the combined pump source test in the holmium doped fibre it was noticed that the 660nm source was producing more MIR light than the 520nm source, from this it was decided to further experiment with the pump sources to try achieve higher levels of IR light. Full spectrum analysis would also be performed where comparisons could be made between the different pump source systems and their wavelength emissions. It was also decided to use a length of 1 meter holmium ZBLAN fibre as it would allow for more absorption from the pump and give higher IR emission readings.

3.7.1 660nm diode as pump source in Ho ZBLAN - 1m

The procedure consisted of the same steps as mentioned previously, with a single 660nm diode acting as the pump source procedures for maximum power in the fibre were performed. From this 85mW of light was detected at the fibres output, maximum fibre absorption procedures were then performed which detected 2.3mW of MIR light from the photoconductor device.

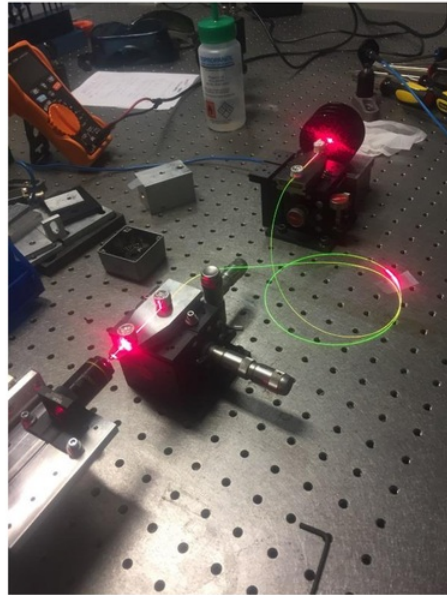


Figure 3.18: 660nm single pump source and fibre aligned for maximum absorption

It is interesting to note the yellow visible light emission seen in Figure 3.18 which occurs around the 577-598nm wavelength and is most probable a product of stimulated emission. Finally OSA's were set up and a sweep of the spectrum was performed from 1000 - 3400 nm, looking at the shorter wavelength emissions we see from Figure 3.19 a small reading around the 1000nm, 1400nm and a peak reading of 44nW around the 1200nm wavelength is evident. An important wavelength emission for Bedrock Photonics research is the 1150nm wavelength which for closer inspection can be seen in Figure 3.20 producing around 12nW at that wavelength.

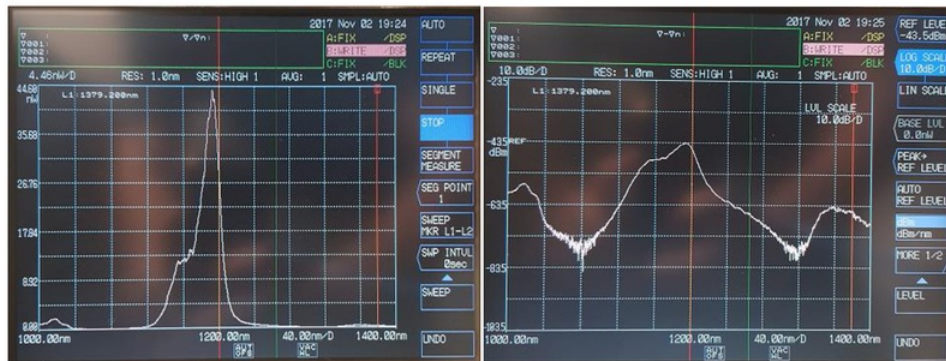


Figure 3.19: 1 - 1.4 μ m spectrum from 660nm pump source linear scale (left), log scale (right)

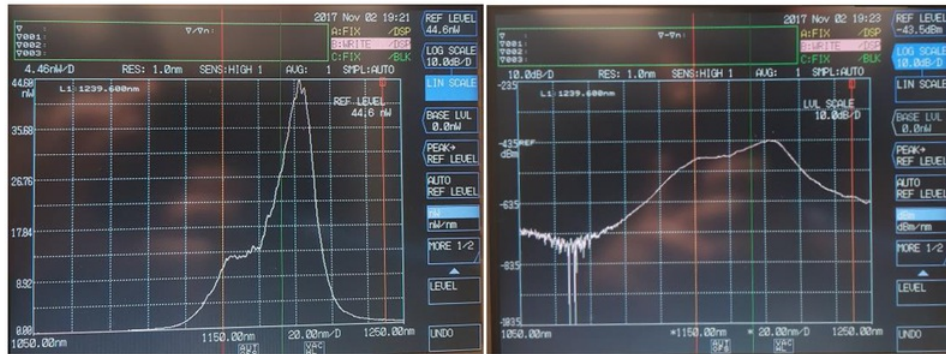


Figure 3.20: Closer inspection of 1150nm wavelength emissions - linear scale (left), log scale (right)

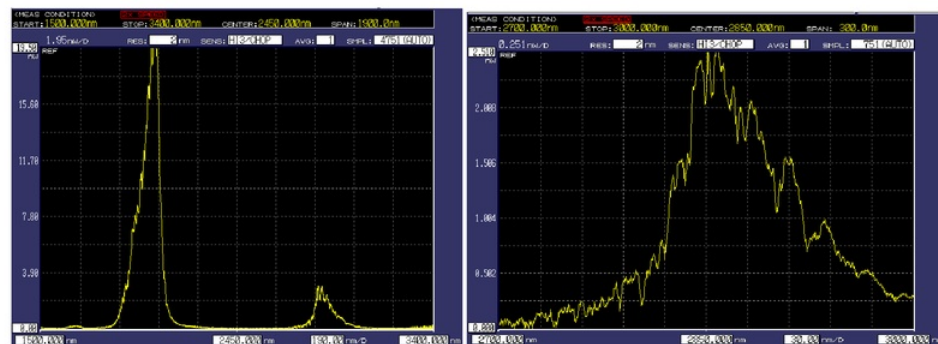


Figure 3.21: The 1.5 - 3.4 μm spectrum (left), closer inspection of 2870nm emissions (right) - linear scale

Finally from Figure 3.21 we see the rest of the spectrum ranging from 1.5 - 3.4 μm , once again the 2870nm mark is of particular importance to Bedrock Photonics, it is also evident that around that mark we are seeing a higher power output that of almost 2nW more than with the combined pump source system Figure 3. 17.

3.7.2 520nm diode as pump source in Ho ZBLAN fibre - 1m

Repeating the same optimizing procedures maximum power output from the fibre was recorded to be 45mW of green light, the maximum absorption procedure gave 0.3mW of IR at the output. Looking at Figure 3. 22 no noticeable changes are observed in the fibre, the light looks similar to it travelling through the SMF-28 non doped fibre, however IR light is not visible and other analyzing methods may reveal something different.

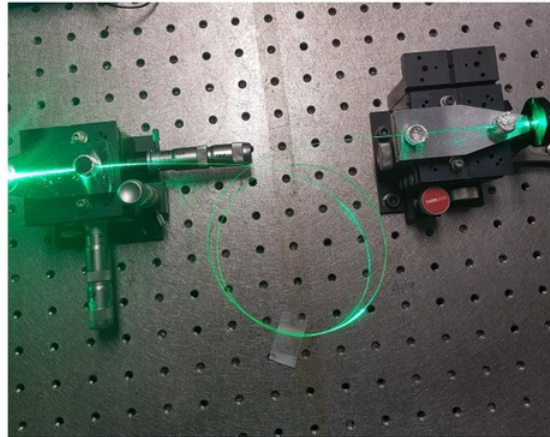


Figure 3.22: Single 520nm pump source in fibre

Provided this the OSA's were once again set up in position and the full spectrum analyzed, referring to Figure 3.23 it is evident similar peaks arise when compared to that of the 660nm single pump source, readings around the 1025nm, 1150nm and 1400nm are detected however it seems the single red pump source produces a more powerful emission. Looking at Figure 3.24 a closer inspection of the 1150nm also shows a similar shape to that of the red, however once again much weaker, the single green pump source produces a 1150nm wavelength at around 300pW compared to the red single pump source giving around 12nW. Looking at the longer wavelengths in Figure 3.25 it would seem the same results are noticeable, there is almost no detection of IR emission around the 2870nm mark and a considerably weaker signal around the 1950nm wavelength which is speculated to be the holmium emission.

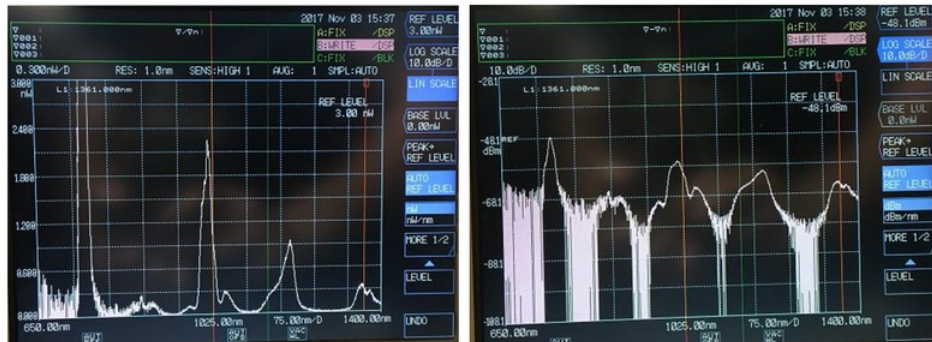


Figure 3.23: Linear scale 650 - 1400nm absorption spectrum (left), log scale (right)

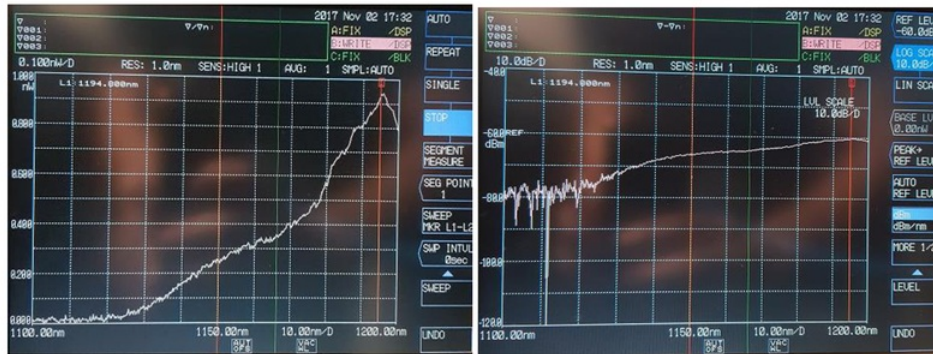


Figure 3.24: Closer inspection of 1150nm wavelength linear scale (left), log scale (right)

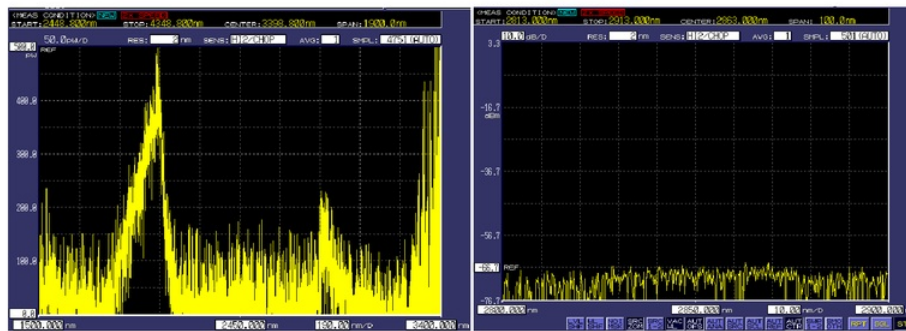


Figure 3.25: The 1.5 - 3.4 μm absorption spectrum in linear scale (left), closer inspection at 2850nm log scale (right)

4 CONCLUSIONS & FUTURE WORK

4.1 Discussion

Throughout the project a successfully created cheap electro-optical system was constructed in which combined the light of the two visible diodes selected. The system also successfully coupled the combined light into doped fibre optic where superluminescent light was detected. The system in question did not only manage the heat of the diodes but also allowed for continuous run time for each diode for periods of up to 5 minutes at a time. There are however many things which could be improved to allow for a more efficient system. Crucial elements to increase the systems efficiency would have to be the diode housing mounts and collimating lenses. A suggestion of spending a bit more money on these components would be advised as precision alignment and optimal power is required for almost all optic related work. Looking at the different pump source systems, it is unfortunate a full view of the spectrum was not attained with both diodes active in the system, however comparing to the single diode pump sources it was noticed that the 660nm light is what mostly influences the level of mid-infrared emission from the holmium ZBLAN fibre. The 660nm diode pump source alone shows a more powerful emission level at the 1150nm and 2870nm wavelengths, even though low it is more intense than the single 520nm diode pump source and combined pump source set ups. It cannot be concluded however that the combined diode pump source is more inefficient than the single diode pump systems as the same tests were not conducted for the combined system. For the single diode systems a longer doped fibre was used and analysis of the full spectrum was performed, however it can be speculated from the low level emission readings that the combined diode pump system gave, this system would in fact be a less efficient system. From this assumption it would be more efficient and cheaper to use the single 660nm diode as a pump source for the system to achieve

stronger emission levels of MIR light, also this way there is less light lost from passing through optical components i.e. dichroic mirror.

4.2 Future Work

From this work the project can go in a number of different directions, for example Bedrock Photonics is particularly interested in the 1150nm and 2870nm wavelength emission the OSA detected, a system could be designed to produce a much stronger emission level for one or both of the mentioned wavelengths. The system could incorporate the cheap temperature sensor/control unit which would monitor the heat created by the diodes, this component was planned to be implemented but was not essential as the heat from the diodes was sufficiently managed. The system could be re-designed to fit in a product casing, the system could be designed to be more compact and robust with some form of internal power supply for a future field use. There are many different directions the project could move onto and with hope it benefits the research field of MIR photonics.

5 APPENDIX

5.1 Datasheets

5.1.1 LPC-840

Under Development
Preliminary

MITSUBISHI LASER DIODES
ML1XX29 SERIES
FOR OPTICAL INFORMATION SYSTEMS

TYPE
NAME

ML101U29

This type is under development. Therefore, please note that this data sheet may be changed without any notice.

DESCRIPTION

ML1XX29 is a high-power, high-efficient AlGaInP semiconductor laser which provides a stable, single transverse mode oscillation with emission wavelength of 660nm and standard pulse light output of 400mW.

ML1XX29 has a real-index-waveguide which improves the slope efficiency (reduction of the operating current) and the astigmatic distance.

Also, ML1XX29 has a window-mirror-facet which improves the maximum output power. That leads to highly reliable and high-power operation at 75 °C.

FEATURES

- High Output Power: 400mW (Pulse)
- High Efficiency: 0.97W/A (typ.)
- Visible Light: 660nm (typ.)
- Low Aspect Ratio ($\delta L / \delta //$): 1.5 (typ.)
- Low Astigmatic Distance: $\leq 1\mu\text{m}$ (typ.)

APPLICATION

Portable High-Density Optical Disc Drives
Re-Writable DVD Drives

ABSOLUTE MAXIMUM RATINGS (Note 1)

Symbol	Parameter	Conditions	Ratings	Unit
Po	Light output power	CW	150	mW
		Pulse(Note 2)	400	
VRL	Reverse voltage	-	2	V
Tc	Case temperature	-	-10 ~ +75	°C
Tstg	Storage temperature	-	-40 ~ +100	°C

Note1: The maximum rating means the limitation over which the laser should not be operated even instant time. This does not mean the guarantee of its lifetime. As for the reliability, please refer to the reliability report issued by Quality Assurance Section, HF & Optical Semiconductor Division, Mitsubishi Electric Corporation.

Note2: TARGET SPEC /Condition Duty Cycle: less than 35%, pulse width: less than 30ns

ELECTRICAL/OPTICAL CHARACTERISTICS (Tc=25°C)

Symbol	Parameter	Test conditions	Min.	Typ.	Max.	Unit
Ith	Threshold current	CW	-	85	-	mA
Iop	Operating current	CW, Po=120mW	-	205	-	mA
Vop	Operating voltage	CW, Po=120mW	-	2.35	3.0	V
η	Slope efficiency	CW, Po=120mW	-	0.97	-	mW/mA
λ_p	Peak wavelength	CW, Po=120mW	654	660	664	nm
$\delta //$	Beam divergence angle (parallel)	CW, Po=120mW	7	10.5	12	°
$\delta \perp$	Beam divergence angle (perpendicular)	CW, Po=120mW	14	16	20	°

5.1.2 NDG7475

NICHIA
Green Laser Diode
NDG7475

[UTZ-SC0339.2]
2013/11/06

Test Sample**■Features**

- Main Transverse Mode
- Can Type: $\phi 9.0$ mm Floating Mounted with Protection device

■Absolute Maximum Ratings

Item	Symbol	Absolute Maximum Ratings	Unit
Forward Current ($T_c=25^\circ\text{C}$)	I_F	(1.8)	A
Allowable Reverse Current ($T_c=25^\circ\text{C}$)	I_R (LD)	85	mA
Storage Temperature	T_{stg}	$-40 \sim 85$	$^\circ\text{C}$
Operating Case Temperature	T_c	$0 \sim 50$	$^\circ\text{C}$

■Initial Electrical/Optical Characteristics $(T_c=25^\circ\text{C})$

Item	Condition	Symbol	Min	Typ	Max	Unit
Optical Output Power	$I_F=1.5\text{A}$	P_o	-	(1.0)	-	W
Dominant Wavelength	$I_F=1.5\text{A}$	λ_d	510	520	525	nm
Threshold Current	CW	I_{th}	-	(0.3)	-	A
Slope Efficiency	CW	η	-	(0.83)	-	W/A
Operating Voltage	$I_F=1.5\text{A}$	V_{op}	-	(4.6)	-	V
Beam Divergence *	Parallel	θ_{\parallel}	5	(11)	25	"
	Perpendicular	θ_{\perp}	35	(46)	55	"
Beam Focusing Accuracy	Perpendicular	$\Delta\theta_{\perp}$	± 5.0	-	± 5.0	"

() are reference figures.

* Full angle at $1/e^2$ from peak intensity.

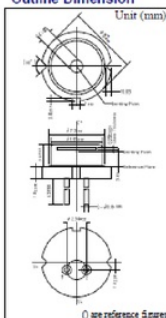
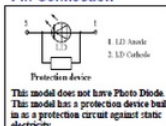
All figures in this specification are measured by Nichia's method and may contain measurement deviations.

This model is Test Sample for evaluation or design purpose only. Life time is not guaranteed.

The above specifications are for reference purpose only and subjected to change without prior notice.

Safety of Laser light

- Laser Light can damage the human eyes and skin. Do not expose the eye or skin to any laser light directly and/or through optical lens. When handling the LDs, wear appropriate safety glasses to prevent laser light, even any reflections from entering to the eye. Focused laser beam through optical instruments will increase the chance of eye hazard.
- These LDs are classified in Class 4 of IEC60825-1 and 21 CFR Part 1040.10 Safety Standards. It is absolutely necessary to take overall safety measures against User's modules, equipment and systems into which Nichia LDs are incorporated and/or integrated.

Outline Dimension**Pin Connection****NICHIA CORPORATION**

<http://www.nichia.co.jp>
<http://www.dglanj.com>

◆ HEADQUARTERS

401 Oka, Kamakura-City, Kanagawa 247-8601, JAPAN
PHONE: +81-884-62211 FAX: +81-884-21035

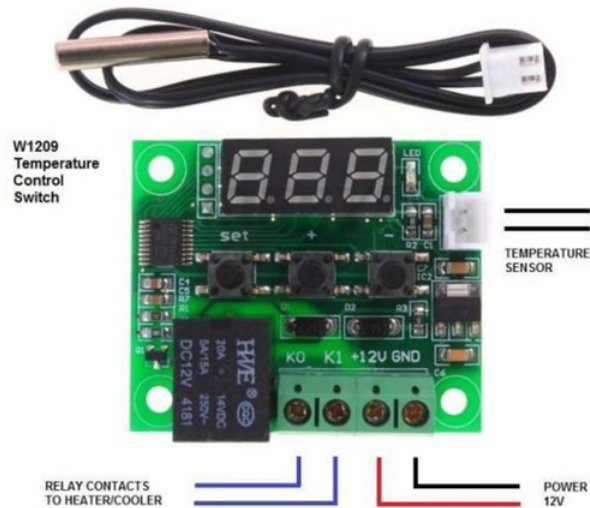
◆ CONTACT

TOKYO SALES OFFICE
15F Tanaka Center Building 34-7, Shiba 5-Chome, Minato-Ku, TOKYO 108-0014, JAPAN
PHONE: +81-3-3456-1102 FAX: +81-3456-0722



5.1.3 W1209

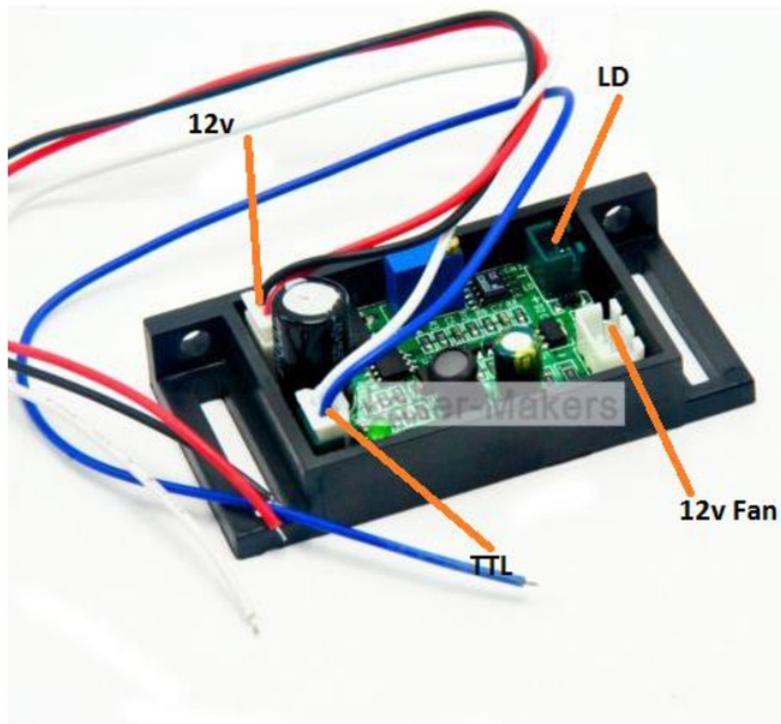
W1209 Temperature Control Switch



DESCRIPTION:

The W1209 is an incredibly low cost yet highly functional thermostat controller. With this module you can intelligently control power to most types of electrical device based on the temperature sensed by the included high accuracy NTC temperature sensor. Although this module has an embedded microcontroller no programming knowledge is required. 3 tactile switches allow for configuring various parameters including on & off trigger temperatures. The on board relay can switch up to a maximum of 240V AC at 5A or 14V DC at 10A. The current temperature is displayed in degrees Centigrade via its 3 digit seven segment display and the current relay state by an on board LED.

5.1.4 DB650-50-500-12V-BL-LM



Specification:

A Driver Circuit board for 650nm 660nm 50-500mw Laser Diode

Input Voltage: 12V

Constant-current drive

With TTL modulation 0-5V 0-20KHZ

Built-in Multiple-turn potentiometer, can adjust the current and control the output power.

5.1.5 DB-12V-200-3500-GD-LM



Specification:

Circuit Control: 12V step-down circuit, constant current output (current and voltage are adjustable)

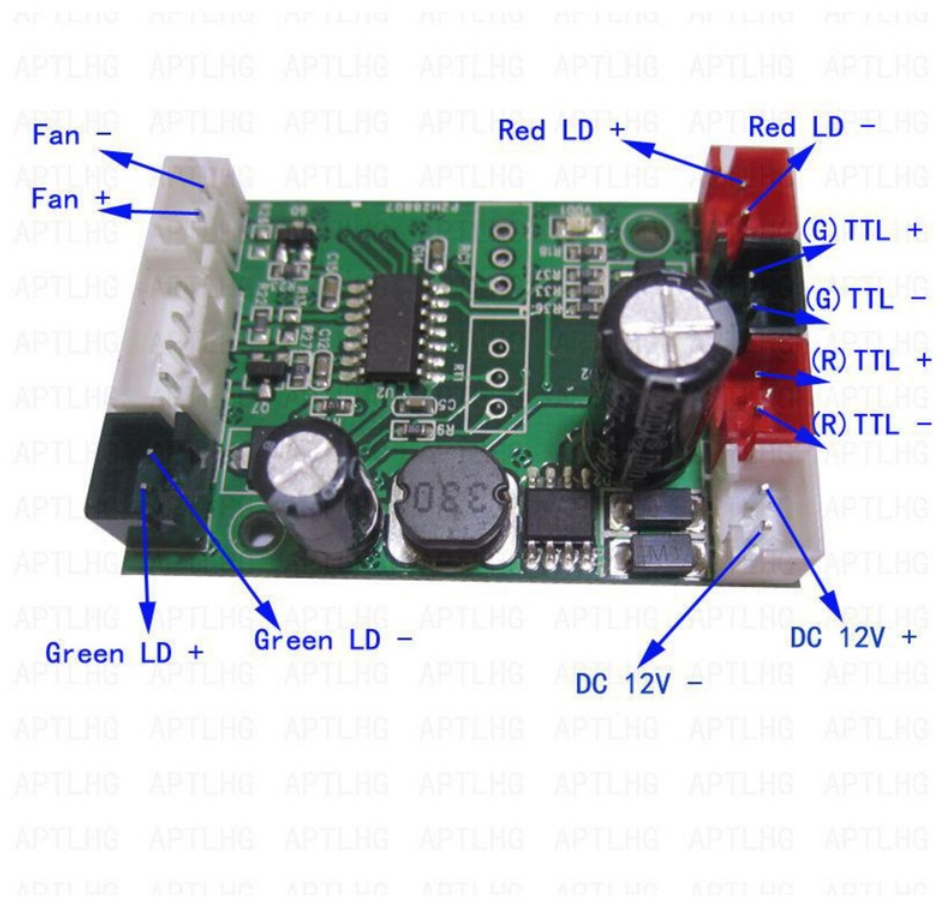
Output Specifications: Max 3A

Scope: 200mW-3.5W 405nm/445nm/450nm/520nm red, green and blue laser drive power

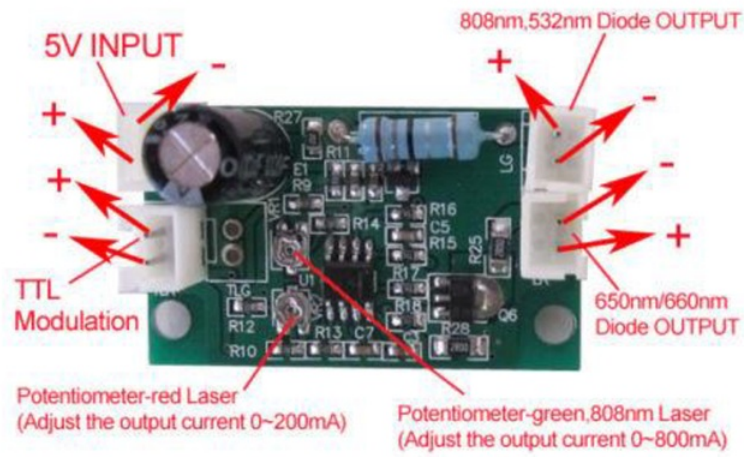
Dimensions: 29x49mmx15.5mm(WxLxH)

Input voltage: 8-14V

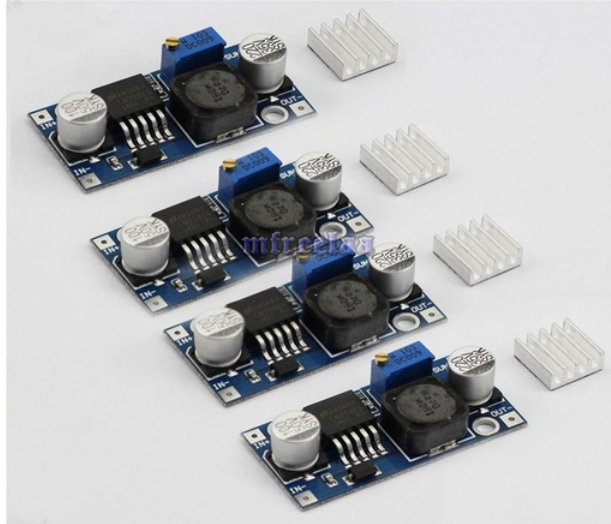
5.1.6 12V-150-500-LD



5.1.7 5V-200-800-GD-RD



5.1.8 LM2596 STEP DOWN REGULATOR



Specifications:

Module property: Non-isolation buck

Rectification mode: non-Synchronous rectifier

Input voltage: DC 4V-40V

Output voltage: DC 1.3V-35V

Output current: Rated current is 2A,maximum 3A(Additional heatsink is required)

Output ripple:30mV(maximum)

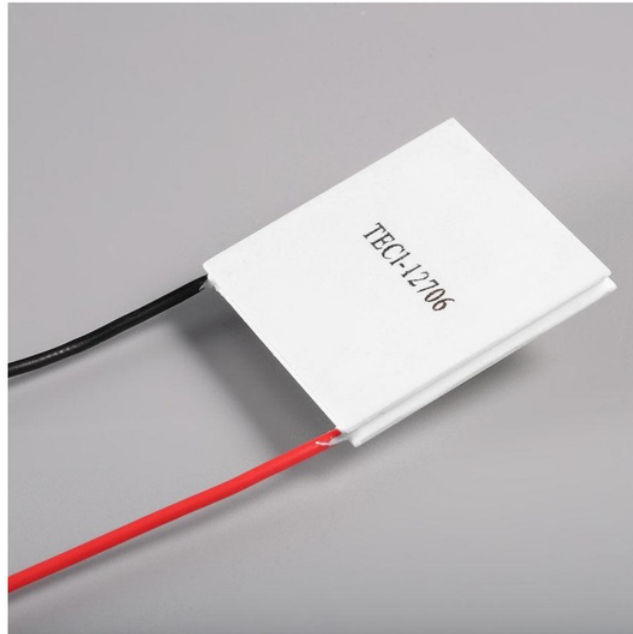
Load regulation:±0.5%

Voltage regulation:± 2.5%

Work temperature:-20°C - +85 °C

Dimension:43mm*21mm*14mm(L*W*H)

5.1.9 TEC1-12706 COOLING PLATE



Specifications:

Model: TEC1-12706

Size: 40mm x 40mm x 4mm

Operates Voltage: 0-12V DC and 0-6A

Operates Temperature: -30c to 70c

Max power consumption: 60 Watts

Original box: NO

Net weight: 22g

Package weight: 31g

Colour: White

5.1.10 Corning SMF-28

Optical Specifications

Attenuation

Standard Attenuation Cells

Wavelength (nm)	Attenuation Cells (dB/km)	
	Premium *	Standard
1310	≤0.35	≤0.40
1550	≤0.25	≤0.30

* Lower attenuation available in limited quantities.

Point Discontinuity

No point discontinuity greater than 0.10 dB at either 1310 nm or 1550 nm.

Attenuation at the Water Peak

The attenuation at 1383 ± 3 nm shall not exceed 2.1 dB/km.

Attenuation vs. Wavelength

Range (nm)	Ref. λ (nm)	Max. α Difference (dB/km)
1285 - 1330	1310	0.05
1525 - 1575	1550	0.05

The attenuation in a given wavelength range does not exceed the attenuation of the reference wavelength (λ) by more than the value α .

Attenuation with Bending

Mandrel Diameter (mm)	Number of Turns	Wavelength (nm)	Induced Attenuation* (dB)
32	1	1550	≤0.50
50	100	1310	≤0.05
50	100	1550	≤0.10

*The induced attenuation due to fiber wrapped around a mandrel of a specified diameter.

Cable Cutoff Wavelength (λ_{ccf})

$\lambda_{ccf} \leq 1260$ nm

Mode-Field Diameter

$9.2 \pm .4$ μ m at 1310 nm

$10.4 \pm .8$ μ m at 1550 nm

Dispersion

Zero Dispersion Wavelength (λ_0):

$1301.5 \text{ nm} \leq \lambda_0 \leq 1321.5 \text{ nm}$

Zero Dispersion Slope (S_0):

$\leq 0.092 \text{ ps}/(\text{nm}^2 \cdot \text{km})$

$$\text{Dispersion} = D(\lambda) \approx \frac{S_0}{4} \left[\lambda - \frac{\lambda_0^4}{\lambda^3} \right] \text{ps}/(\text{nm} \cdot \text{km}),$$

for $1200 \text{ nm} \leq \lambda \leq 1600 \text{ nm}$

λ = Operating Wavelength

Polarization Mode Dispersion

Fiber Polarization Mode Dispersion (PMD)

	Value (ps/ $\sqrt{\text{km}}$)
PMD Link Value	≤ 0.1*
Maximum Individual Fiber	≤ 0.2

* Complies with IEC SC 86A/WG1, Method 1, September 1997.

The PMD link value is a term used to describe the PMD of concatenated lengths of fiber (also known as the link quadrature average). This value is used to determine a statistical upper limit for system PMD performance.

Individual PMD values may change when cabled. Corning's fiber specification supports emerging network design requirements for a 0.5 ps/ $\sqrt{\text{km}}$ maximum PMD.

Environmental Specifications

Environmental Test Condition	Induced Attenuation (dB/km)	
	1310 nm	1550 nm
Temperature Dependence -60°C to +85°C*	≤ 0.05	≤ 0.05
Temperature-Humidity Cycling -10°C to +85°C*, up to 98% RH	≤ 0.05	≤ 0.05
Water Immersion, 23°C ± 2°C*	≤ 0.05	≤ 0.05
Heat Aging, 85°C ± 2°C*	≤ 0.05	≤ 0.05

*Reference temperature = +23°C

Operating Temperature Range -60°C to +85°C

Dimensional Specifications

Standard Length (km/reel): 2.2 - 25.2*

* Longer spliced lengths available at a premium.

Glass Geometry

Fiber Curl: ≥ 4.0 m radius of curvature

Cladding Diameter: 125.0 ± 1.0 μm

Core-Clad Concentricity: ≤ 0.5 μm

Cladding Non-Circularity: $\leq 1.0\%$

Defined as: $\left[1 - \frac{\text{Min. Cladding Diameter}}{\text{Max. Cladding Diameter}} \right] \times 100$

Coating Geometry

Coating Diameter: 245 ± 5 μm

Coating-Cladding Concentricity: < 12 μm

Mechanical Specifications

Proof Test

The entire fiber length is subjected to a tensile proof stress ≥ 100 kpsi (0.7 GN/m^2)*.

* Higher proof test levels available at a premium.

Performance Characterizations

Characterized parameters are typical values.

Core Diameter: 8.2 μm

Numerical Aperture: 0.14

NA is measured at the one percent power level of a one-dimensional far-field scan at 1310 nm.

Zero Dispersion Wavelength (λ_0): 1312 nm

Zero Dispersion Slope (S_0): 0.090 ps/(nm²•km)

Refractive Index Difference: 0.36%

Effective Group Index of Refraction (N_{eff}):

1.4677 at 1310 nm

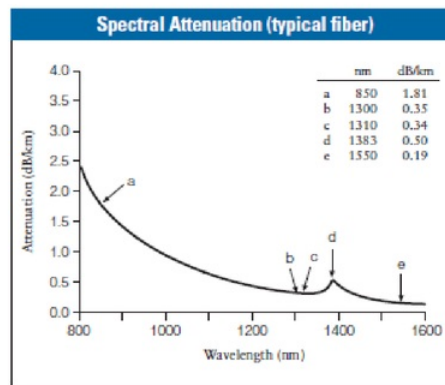
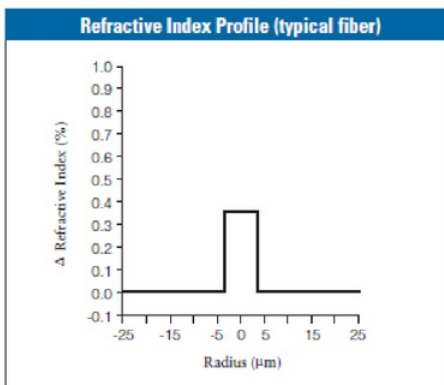
1.4682 at 1550 nm

Fatigue Resistance Parameter (n_d): 20

Coating Strip Force:

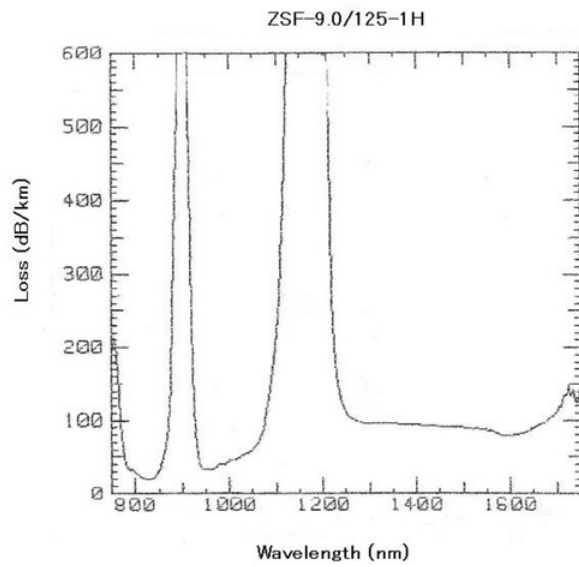
Dry: 0.6 lbs (2.7 N)

Wet, 14-day room temperature: 0.6 lbs (2.7 N)



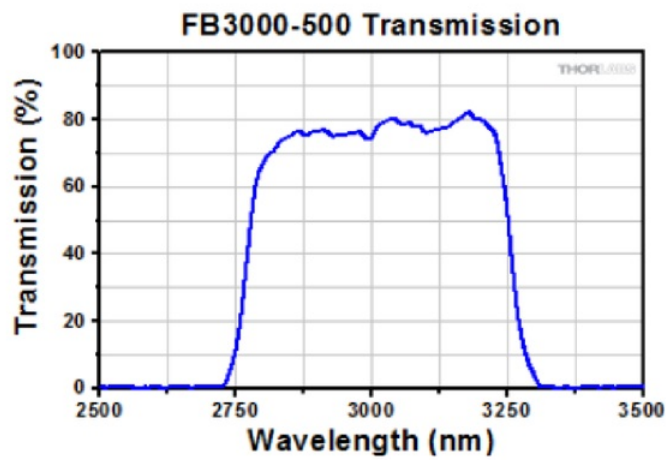
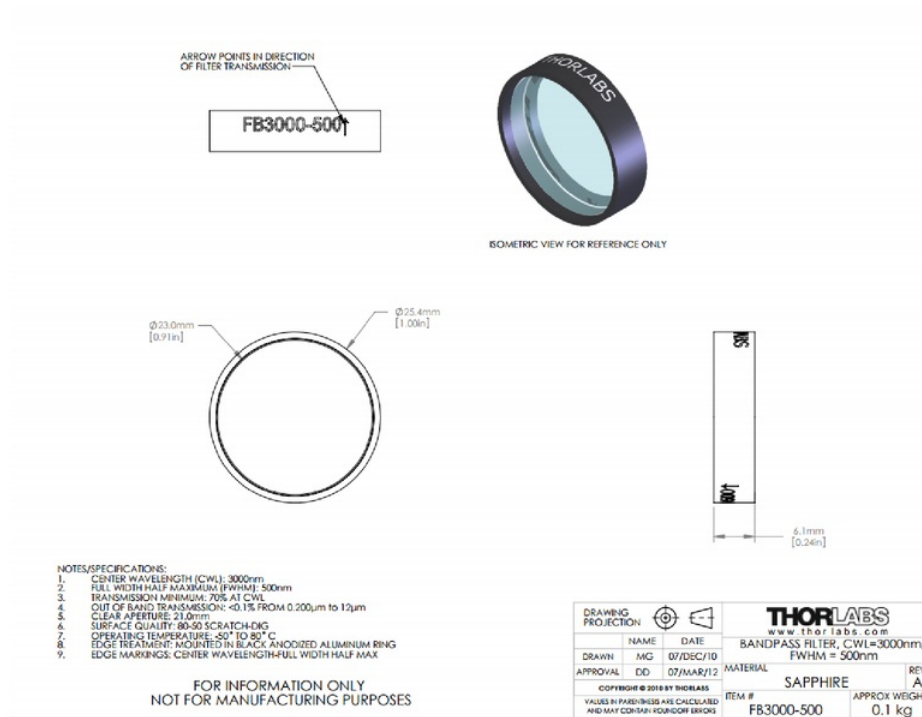
5.1.11 Holmium ZBLAN

Loss Spectrum:



Item	Dopant	Concentration	NA	Core	Cladding	Coating	Cut-off
ZSF-9/125	Ho	1000ppm mol	0.16 μm	9 μm	125 μm	450 μm	<2100

5.1.12 FB3000-500



5.1.13 LM317 current-limiter circuit



LM317

SLVS044X – SEPTEMBER 1997 – REVISED SEPTEMBER 2016

LM317 3-Terminal Adjustable Regulator

1 Features

- Output Voltage Range Adjustable From 1.25 V to 37 V
- Output Current Greater Than 1.5 A
- Internal Short-Circuit Current Limiting
- Thermal Overload Protection
- Output Safe-Area Compensation

2 Applications

- ATCA Solutions
- DLP: 3D Biometrics, Hyperspectral Imaging, Optical Networking, and Spectroscopy
- DVR and DVS
- Desktop PC
- Digital Signage and Still Camera
- ECG Electrocardiogram
- EV HEV Charger: Level 1, 2, and 3
- Electronic Shelf Label
- Energy Harvesting
- Ethernet Switch
- Femto Base Station
- Fingerprint and Iris Biometrics
- HVAC: Heating, Ventilating, and Air Conditioning
- High-Speed Data Acquisition and Generation
- Hydraulic Valve
- IP Phone: Wired and Wireless
- Intelligent Occupancy Sensing
- Motor Control: Brushed DC, Brushless DC, Low-Voltage, Permanent Magnet, and Stepper Motor
- Point-to-Point Microwave Backhaul
- Power Bank Solutions
- Power Line Communication Modem
- Power Over Ethernet (PoE)
- Power Quality Meter
- Power Substation Control
- Private Branch Exchange (PBX)
- Programmable Logic Controller
- RFID Reader
- Refrigerator
- Signal or Waveform Generator
- Software Defined Radio (SDR)
- Washing Machine: High-End and Low-End
- X-ray: Baggage Scanner, Medical, and Dental

3 Description

The LM317 device is an adjustable three-terminal positive-voltage regulator capable of supplying more than 1.5 A over an output-voltage range of 1.25 V to 37 V. It requires only two external resistors to set the output voltage. The device features a typical line regulation of 0.01% and typical load regulation of 0.1%. It includes current limiting, thermal overload protection, and safe operating area protection. Overload protection remains functional even if the ADJUST terminal is disconnected.

Device Information⁽¹⁾

PART NUMBER	PACKAGE	BODY SIZE (NOM)
LM317DCY	SOT-223 (4)	6.50 mm × 3.50 mm
LM317KCS	TO-220 (3)	10.16 mm × 9.15 mm
LM317KCT	TO-220 (3)	10.16 mm × 8.59 mm
LM317KTT	TO-263 (3)	10.16 mm × 9.01 mm

(1) For all available packages, see the orderable addendum at the end of the data sheet.

8.3.3 Precision Current-Limiter Circuit

This application limits the output current to the I_{LIMIT} in the diagram.

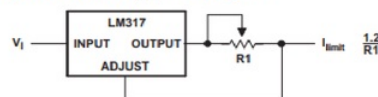


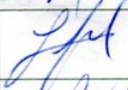












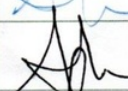

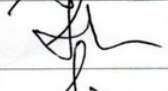

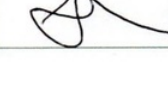






Figure 14. Precision Current-Limiter Circuit

Copyright © 2016, Texas Instruments Incorporated

5.2 Consultation Meetings Attendance Form

Consultation Meetings Attendance Form

Week	Date	Comments (if applicable)	Student's Signature	Supervisor's Signature
2	29/7/2017	Start of project		
3	6/8/2017	debrief		
4	12/8/2017			
5	20/8/2017			
6	24/8/2017			
7	5/9/2017			
8	1/10/2017			
9	8/10/2017			
10	14/10/2017			
11	21/10/2017			
12	27/10/2017			
13	2/11/2017			

6 BIBLIOGRAPHY

- [1] E. Mujic, "The development of a compact and commercial tuneable 3um fibre laser," Ph.D. dissertation, University of Sydney School of Physics, 2013.
- [2] J. W. Hazey, V. K. Narula, D. B. Renton, K. M. Reavis, C. M. Paul, K. E. Hinshaw, P. Muscarella, E. C. Ellison, and W. S. Melvin, "Natural-orifice transgastric endoscopicperitoneoscopy in humans: Initial clinical trial," *Surgical Endoscopy*, vol. 22, no. 1, pp. 16-20, 2007.
- [3] F. McAleavey, J. O'Gorman, J. Donegan, B. MacCraith, J. Hegarty, and G. Maze, "Narrow linewidth, tunable $\text{tm}/\text{sup } 3+/-$ -doped fluoride fibre laser for optical-based hydrocarbon gas sensing," *IEEE J. Select. Topics Quantum Electron.*, vol. 3, no. 4, pp. 1103-1111, 1997.
- [4] G. M. Peavy, L. Reinisch, J. T. Payne, and V. Venugopalan, "Comparison of cortical bone ablations by using infrared laser wavelengths 2.9 to 9.2 um," *Lasers Surg. Med.*, vol. 25, no. 5, pp. 421-434, 1999.
- [5] M. C. Pierce, S. D. Jackson, M. R. Dickinson, T. A. King, and P. Sloan, "Laser-tissue interaction with a continuous wave 3-um fibre laser: Preliminary studies with soft tissue," *Lasers Surg. Med.*, vol. 26, no. 5, pp. 491-495, 2000.
- [6] T. Sumiyoshi, H. Sekita, T. Arai, S. Sato, M. Ishihara, and M. Kikuchi, "High-power continuous-wave 3- and 2-m cascade $\text{ho}/\text{sup } 3+/-$:zblanfiber laser and its medical applications," *IEEE J. Select. Topics Quantum Electron.*, vol. 5, no. 4, pp. 936-943, 1999.
- [7] E. Cook, "Drive current control and forced-air cooling of high power semiconductor diode lasers," Bachelor of Engineering dissertation, Macquarie University, 2015.

- [8]"Spectroscopy". En.wikipedia.org. N.p. [Accessed: 24- May- 2017].
- [9]Libbrecht, Professor Kenneth. Diode Laser Spectroscopy. 1st ed. 2011. Print pp1-4.
- [10] J. El-Azab. National Institute of Laser Enhanced Sciences, 2012. [Online]. Available: <http://niles.cu.edu.eg/courses/EAL503 FALL 2012/Semiconductor photon sources.pdf>
- [11] "Semiconductor Lasers | Types, Applications, Construction, Working, Advantages And Disadvantages". Daenotes.com. N.p., 2017
- [12] J. Lazar, "Laser diode current controller with a high level of protection against electromagnetic interference," Rev. Sci. Instrum., vol. 74, no. 8, p. 3816, 2003.
- [13] Lee, H. (2010). Thermal design. Hoboken: Wiley, pp. 34-99.
- [14] Aavid Engineering, Inc., EDS #117, Interface Materials, January 1992.
- [15] R.A. Wirtz, W. Chen, and R. Zhou, Effect of Flow Bypass on the Performance of Longitudinal Fin Heat Sinks, ASME Journal of Electronic Packaging", Vol.~116,pp.~206-211,1994.
- [16] S. Lee, Optimum Design and Selection of Heat Sinks, Proceedings of 11th IEEE Semi-Therm Symposium, pp. 48-54, 1995.
- [17] S. Song, S. Lee, and V. Au, Closed Form Equation for Thermal Constriction/Spreading Resistances with Variable Resistance Boundary Condition, Proceedings of the 1994 IEPS Technical Conference, pp. 111-121,1994.
- [18] Sudhanshu Sharma , V. K. Dwivedi & S. N. Pandit (2014) A Review of Thermoelectric Devices for Cooling Applications, International Journal of Green Energy, 11:9, 899-909, access : <http://dx.doi.org/10.1080/15435075.2013.829778>
- [19] Y.-W. Chang, C.-C. Chang, M.-T. Ke, and S.-L. Chen, \Thermoelectric air-cooling module for electronic devices," Applied Thermal Engineering, vol. 29, no. 13, pp. 2731-2737, 2009.
- [20] Paschotta, Dr. "Encyclopedia Of Laser Physics And Technology - Beam Combining, Coherent, Incoherent, Spectral, High-Power Laser, Power Scaling, Amplifiers". Rp-photonics.com. N.p.
- [21]Clarke, Roy. "Techniques For Laser Combining". Innovations Live 2 (2015): 2. Web

- [22] Lowenthal, Dennis, Brown, Andrew NASA Tech Briefs " Spectral vs. Coherent Beam Combining: How Do They Compare?";Jan 2006; 30, 1; SciTech Premium Collection, pp. 10A
- [23] R. Eason, \How fibre lasers work | optoelectronics research centre | university of southampton," 2015. [Online]. Available: <http://www.orc.soton.ac.uk/61.html>
- [24] R. Paschotta, article on 'superluminescence' in the Encyclopedia of Laser Physics and Technology, [Online]. Available: <https://www.rp-photonics.com/superluminescence.html>
- [25] T. Ackroyd, "Implementation of an automated diffraction grating tuner for a tuneable fibre laser," Bachelor of Engineering dissertation, Macquarie University, 2015.